The CGM around Massive Galaxies at z=2-3: A Test for Stellar Feedback, Galactic Outflows and Cold Streams

Sijing Shen
UC Santa Cruz/IMPS Fellow

The Baryon Cycle Conference, Irvine, CA June 14, 2012

In collaboration with: Piero Madau, Javiera Guedes, Anthony Aguirre, Jason X. Prochaska, James Wadsley & Lucio Mayer

Southern California CCGE Center for Galaxy Evolution

UC-HiPACC

The CGM-Galaxy Interactions: The Baryon Cycle

The CGM-Galaxy Interactions: The Baryon Cycle

- Galactic outflows

- Galactic outflows observed in local starburst with v ~ hundreds km/s (e.g., Shapley+2003; Veilleux+2005; Weiner+2009)

The CGM-Galaxy Interactions: The Baryon Cycle

- Galactic outflows

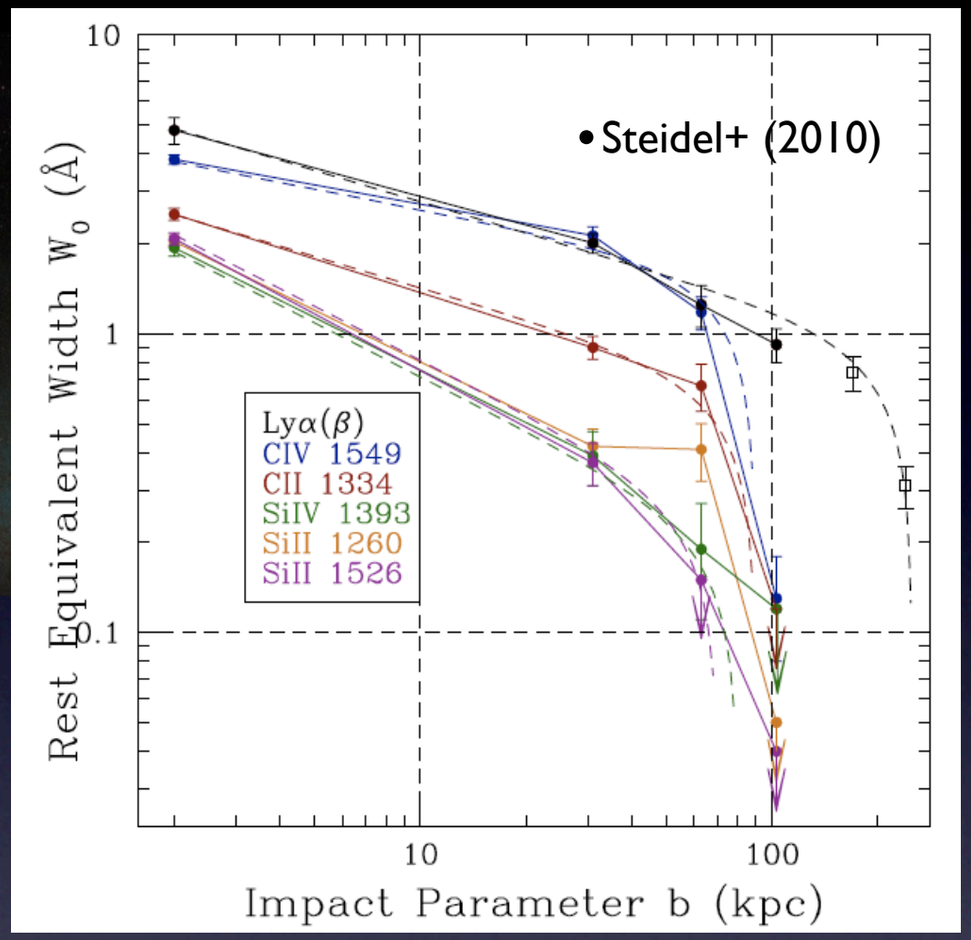

- Galactic outflows observed in local starburst with v ~ hundreds km/s (e.g., Shapley+2003; Veilleux+2005; Weiner+2009)
- Far-UV spectra of angular pairs of galaxies/ quasar-galaxies provides detailed map of the CGM metals (Steidel+2010) at higher z
- Increasing amount of data about the CGM at low redshift (e.g., Prochaska & Hennawi 2009; Chen +2010; Crighton+2011; Prochaska+2011; Tumlinson +2012; Werk+2012)

The CGM-Galaxy Interactions: The Baryon Cycle

- Galactic outflows

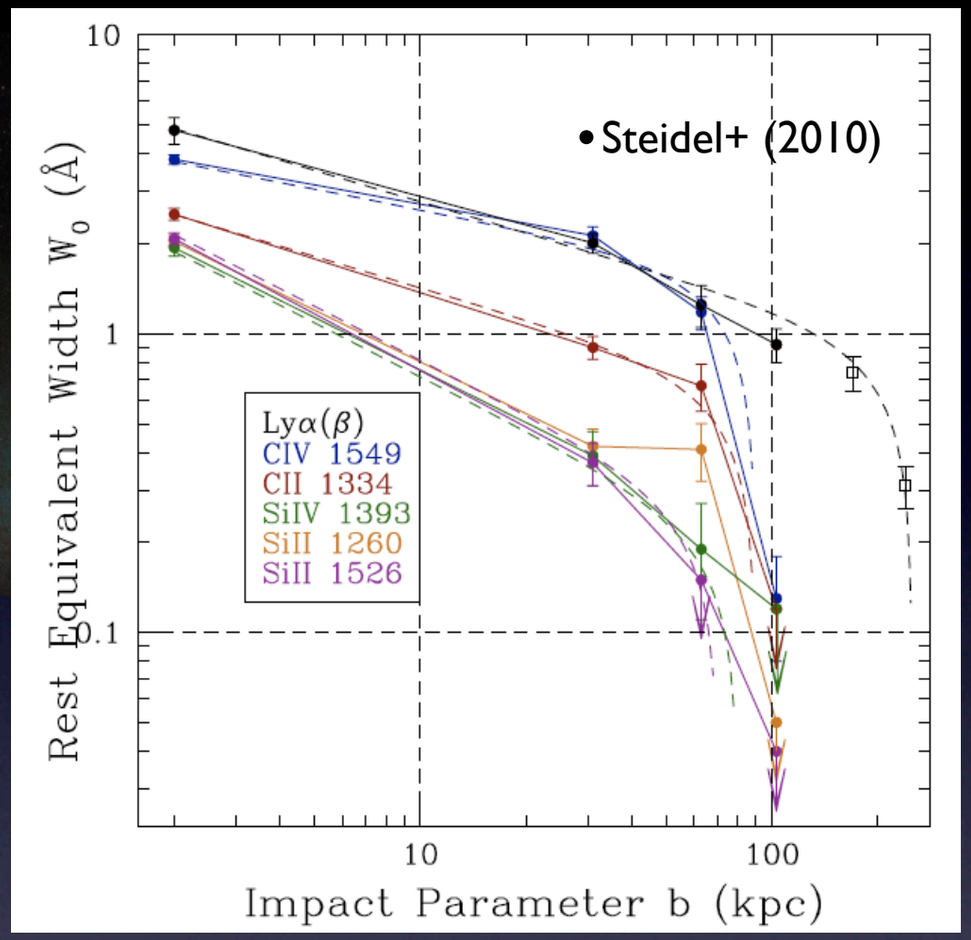

Gas from IGM inflows into galactic halos

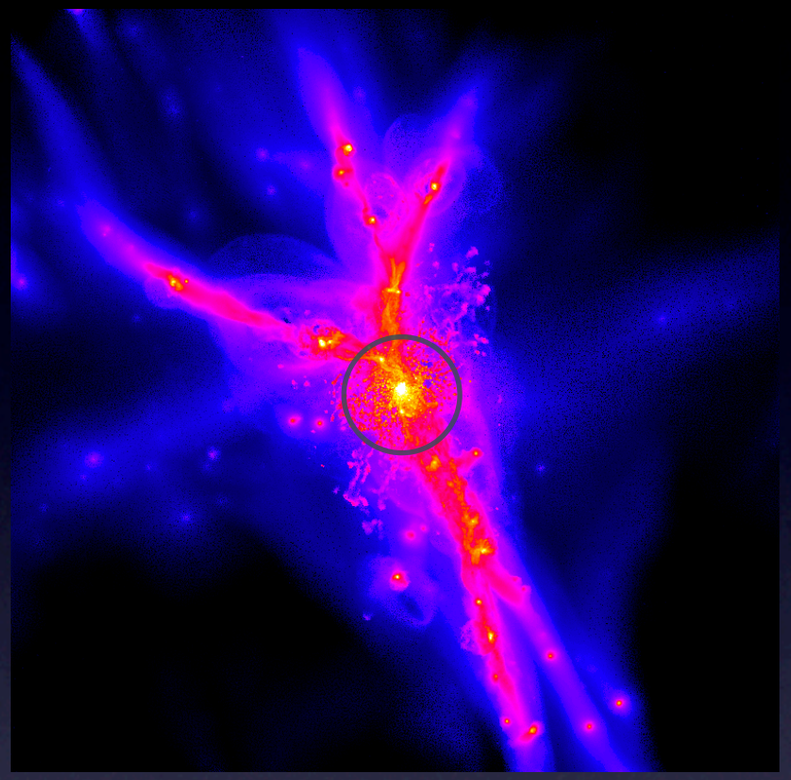

- Galactic outflows observed in local starburst with v ~ hundreds km/s (e.g., Shapley+2003; Veilleux+2005; Weiner+2009)
- Far-UV spectra of angular pairs of galaxies/ quasar-galaxies provides detailed map of the CGM metals (Steidel+2010) at higher z
- Increasing amount of data about the CGM at low redshift (e.g., Prochaska & Hennawi 2009; Chen +2010; Crighton+2011; Prochaska+2011; Tumlinson +2012; Werk+2012)

The CGM-Galaxy Interactions: The Baryon Cycle

- Galactic outflows

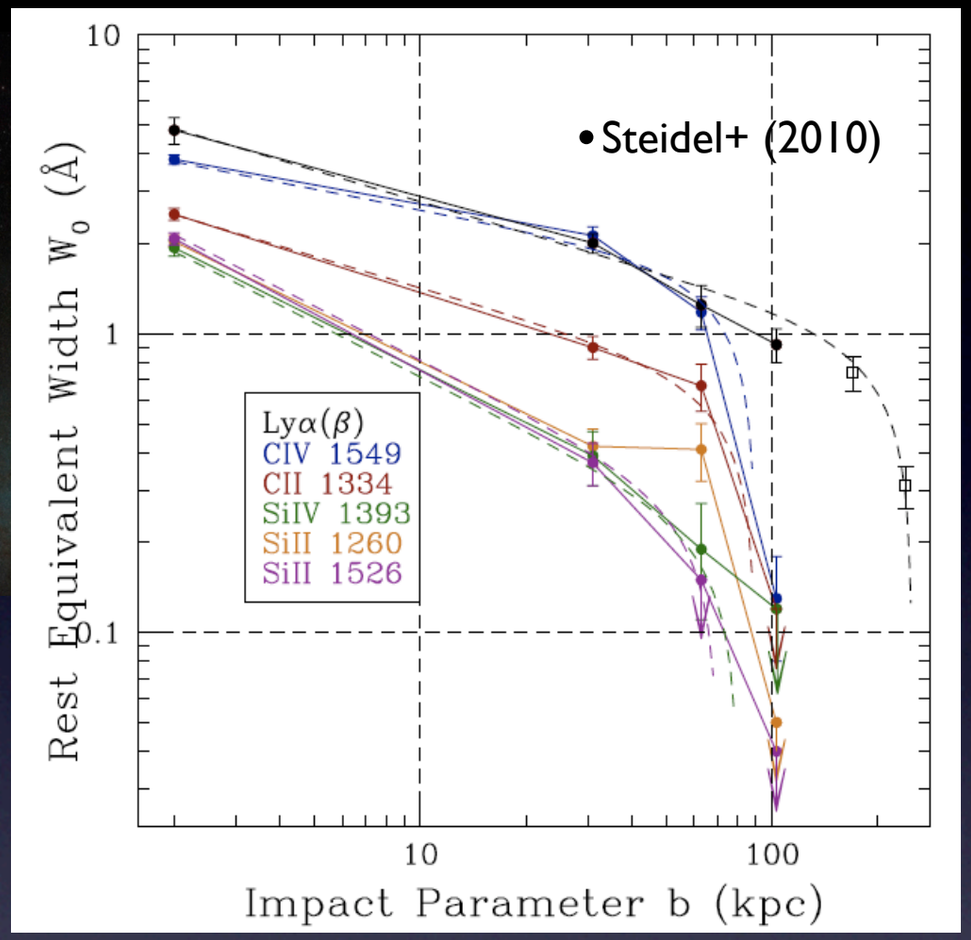

- Galactic outflows observed in local starburst with v ~ hundreds km/s (e.g., Shapley+2003; Veilleux+2005; Weiner+2009)
- Far-UV spectra of angular pairs of galaxies/ quasar-galaxies provides detailed map of the CGM metals (Steidel+2010) at higher z
- Increasing amount of data about the CGM at low redshift (e.g., Prochaska & Hennawi 2009; Chen +2010; Crighton+2011; Prochaska+2011; Tumlinson +2012; Werk+2012)

Gas from IGM inflows into galactic halos

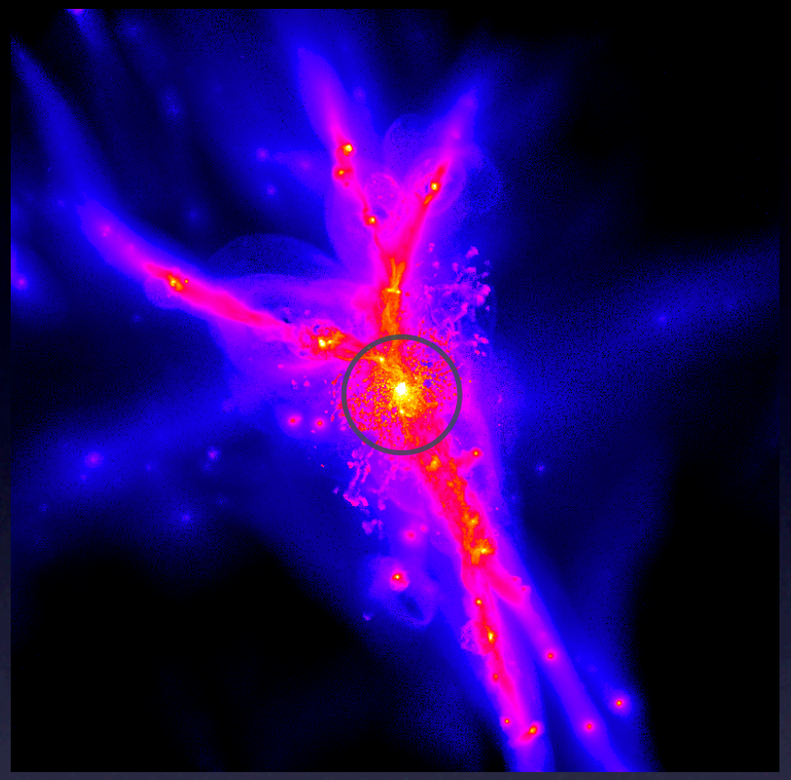

- At high z, "cold" accretion mode dominates (e.g., Kereš+ 2005, 2009; Dekel & Birnboim 2006; Ocvirk+2008)
- Prediction of cold stream detection

  1. statistical prescription using cosmological volumes (e.g., Dekel+2009; van de Voort+2012)

  2. zoom-in simulations that do not generate strong outflows(e.g., Fumagalli + 2011; Faucher-Giguère & Kereš 2011; Kimm +2011; Stewart+2011)

The CGM-Galaxy Interactions

Our (not complete at all) wish list:

The CGM-Galaxy Interactions

Our (not complete at all) wish list:

- Can the observed properties, such as the W_0-b and $N_{HI(OVI)}$-b relation, or HI covering factors be reproduced by simulations of galaxy formation?

The CGM-Galaxy Interactions

Our (not complete at all) wish list:

- Can the observed properties, such as the W_0-b and $N_{HI(OVI)}$-b relation, or HI co factors be reprod simulations of g formation

- What can we say about the ionization & thermal state, kinematics, spacial distribution of the CGM from observed data?

The CGM-Galaxy Interactions

Our (not complete at all) wish list:

- Can the observed properties, such as the W_0-b and $N_{HI(OVI)}$-b relation, or HI co factors be reprod simulations of g formation

- What can we say about the ionization & thermal state, kinematics, spacial distribution of from observe

- How the inflows and outflows affect each other? Are inflows enriched? Can we differentiate inflow and outflow gas by its metallicity?

The CGM-Galaxy Interactions

Our (not complete at all) wish list:

- Can the observed properties, such as the W_0-b and $N_{HI(OVI)}$-b relation, or HI co factors be reprod simulations of g formation

- What can we say about the ionization & thermal state, kinematics, spacial distribution of from observe

- How do various properties of the CGM depend on the stellar mass of galaxies, the SFR, environment?

- How the inflows and outflows affect each other? Are inflows enriched? Can we differentiate inflow and outflow gas by its metallicity?

The CGM-Galaxy Interactions

Our (not complete at all) wish list:

- Can the observed properties, such as the W_0-b and $N_{HI(OVI)}$-b relation, or HI co factors be reprod simulations of g formation
- What can we say about the ionization & thermal state, kinematics, spacial distribution of from observ
- How do various properties of the CGM depend on the stellar mass of galaxies, the SFR, environment?
- How does the CGM and its metals evolve with time?
- How the inflows and outflows affect each other? Are inflows enriched? Can we differentiate inflow and outflow gas by its metallicity?

The CGM-Galaxy Interactions

Our (not complete at all) wish list:

- Can the observed properties, such as the W_0-b and $N_{HI(OVI)}$-b relation, or HI co factors be reprod simulations of g formation
- What can we say about the ionization & thermal state, kinematics, spacial distribution of from observe
- How do various properties of the CGM depend on the stellar mass of galaxies, the SFR, environment?
- How the inflows and outflows affect each other? Are inflows enriched? Can we differentiate inflow and outflow gas by its metallicity?
- How does the CGM and its metals evolve with time?

...

The Eris2 Simulation

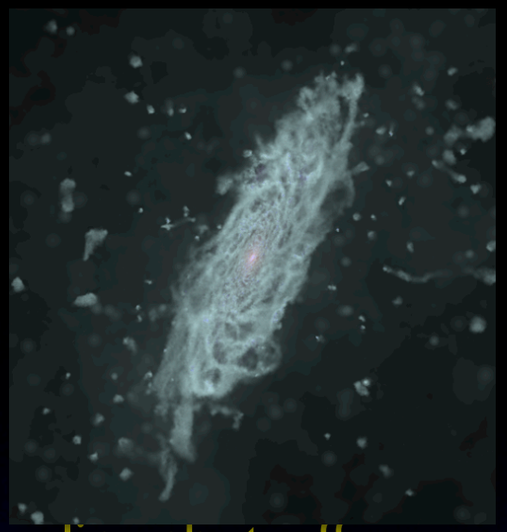

- TreeSPH code Gasoline (Wadsley et al. 2004)
- SF: $d\rho_*/dt = \varepsilon_{SF}\rho_{gas}/t_{dyn} \propto \rho_{gas}^{1.5}$ when gas has $n_H > n_{SF}$
- Blastwave feedback model for SN II (Stinson+ 2006): radiative cooling shut-off according to analytical solution from McKee & Ostriker (1977).
- Radiative cooling for H, He and metals were computed using Cloudy (Ferland+ 1998), assuming ionization equilibrium under uniform UVB (Haardt & Madau 2012)
- Turbulent diffusion model (Wadsley+ 2008; Shen+2010) to capture mixing of metals in turbulent outflows.
- Same initial set up as in Eris (Guedes+2011)

Galaxy	m_{DM} (Ms)	m_{SPH} (Ms)	ε_G (pc)	n_{SF} (cm^{-3})
Eris2	9.8×10^4	2×10^4	120	20.0

The Eris2 Simulation

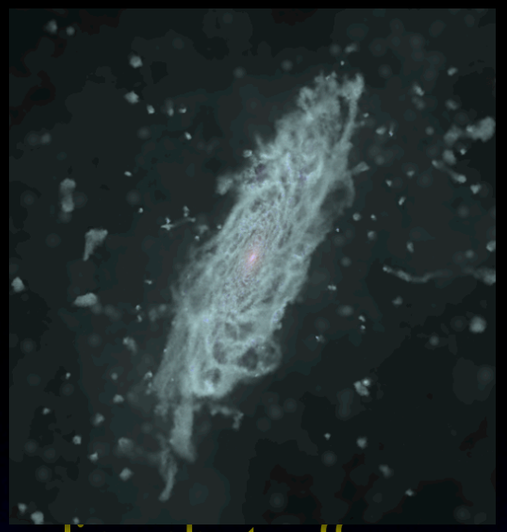

- TreeSPH code Gasoline (Wadsley et al. 2004)
- SF: $d\rho_*/dt = \varepsilon_{SF}\rho_{gas}/t_{dyn} \propto \rho_{gas}^{1.5}$ when gas has $n_H > n_{SF}$
- Blastwave feedback model for SN II (Stinson+ 2006): radiative cooling shut-off according to analytical solution from McKee & Ostriker (1977).
- Radiative cooling for H, He and metals were computed using Cloudy (Ferland+ 1998), assuming ionization equilibrium under uniform UVB (Haardt & Madau 2012)
- Turbulent diffusion model (Wadsley+ 2008; Shen+2010) to capture mixing of metals in turbulent outflows.
- Same initial set up as in Eris (Guedes+2011)

Galaxy	m_{DM} (Ms)	m_{SPH} (Ms)	ε_G (pc)	n_{SF} (cm^{-3})
Eris2	9.8×10^4	2×10^4	120	20.0

Very high resolution - 4 M particles within Rvir at z =2.8, to resolve the galaxy structure, the progenitor satellites and dwarfs

The Eris2 Simulation

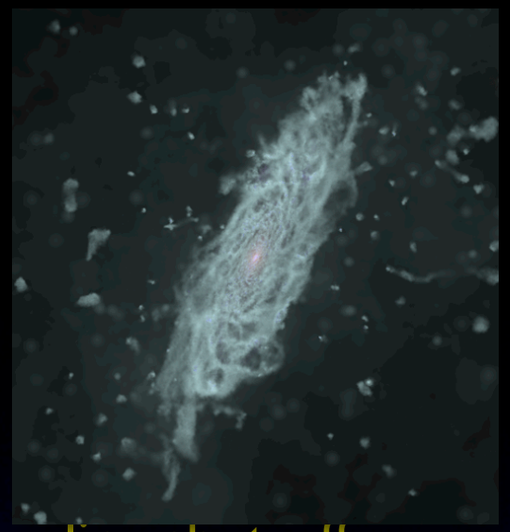

- TreeSPH code Gasoline (Wadsley et al. 2004)
- SF: $d\rho_*/dt = \varepsilon_{SF}\rho_{gas}/t_{dyn} \propto \rho_{gas}^{1.5}$ when gas has $n_H > n_{SF}$
- Blastwave feedback model for SN II (Stinson+ 2006): radiative cooling shut-off according to analytical solution from McKee & Ostriker (1977).
- Radiative cooling for H, He and metals were computed using Cloudy (Ferland+ 1998), assuming ionization equilibrium under uniform UVB (Haardt & Madau 2012)
- Turbulent diffusion model (Wadsley+ 2008; Shen+2010) to capture mixing of metals in turbulent outflows.
- Same initial set up as in Eris (Guedes+2011)

Galaxy	m_{DM} (Ms)	m_{SPH} (Ms)	ε_G (pc)	n_{SF} (cm^{-3})
Eris2	9.8×10^4	2×10^4	120	20.0

Very high resolution - 4 M particles within Rvir at z =2.8, to resolve the galaxy structure, the progenitor satellites and dwarfs

High SF threshold, allow the inhomogeneous SF site to be resolved and localize feedback

Eris2 and Its Metal-Enriched CGM at z = 2.8

$M_{vir}(M_{sun})$	R_{vir} (kpc)	$M^*(M_{sun})$	SFR(M_s/yr)	12+log(O/H)	$T>10^5$ K (%)	R_z	$\langle Zg \rangle_{vir}$
2.6×10^{11}	50	1.5×10^{10}	20	8.50	54%	~5 Rvir	0.7 Z_{sun}

- At z=2.8, Eris2 has M_{vir} and M_* close to an LBG but lower than typical observed LBGs (e.g, Steidel+ 2010)
- More than half of metals locked in the warm-hot ($T > 10^5$) phase
- Cold, SF gas has 12+log(O/H)=8.5, within the M_*-Z relationship (Erb +2006)
- The metal "bubble" extends up to 250 kpc, 5 Rvir

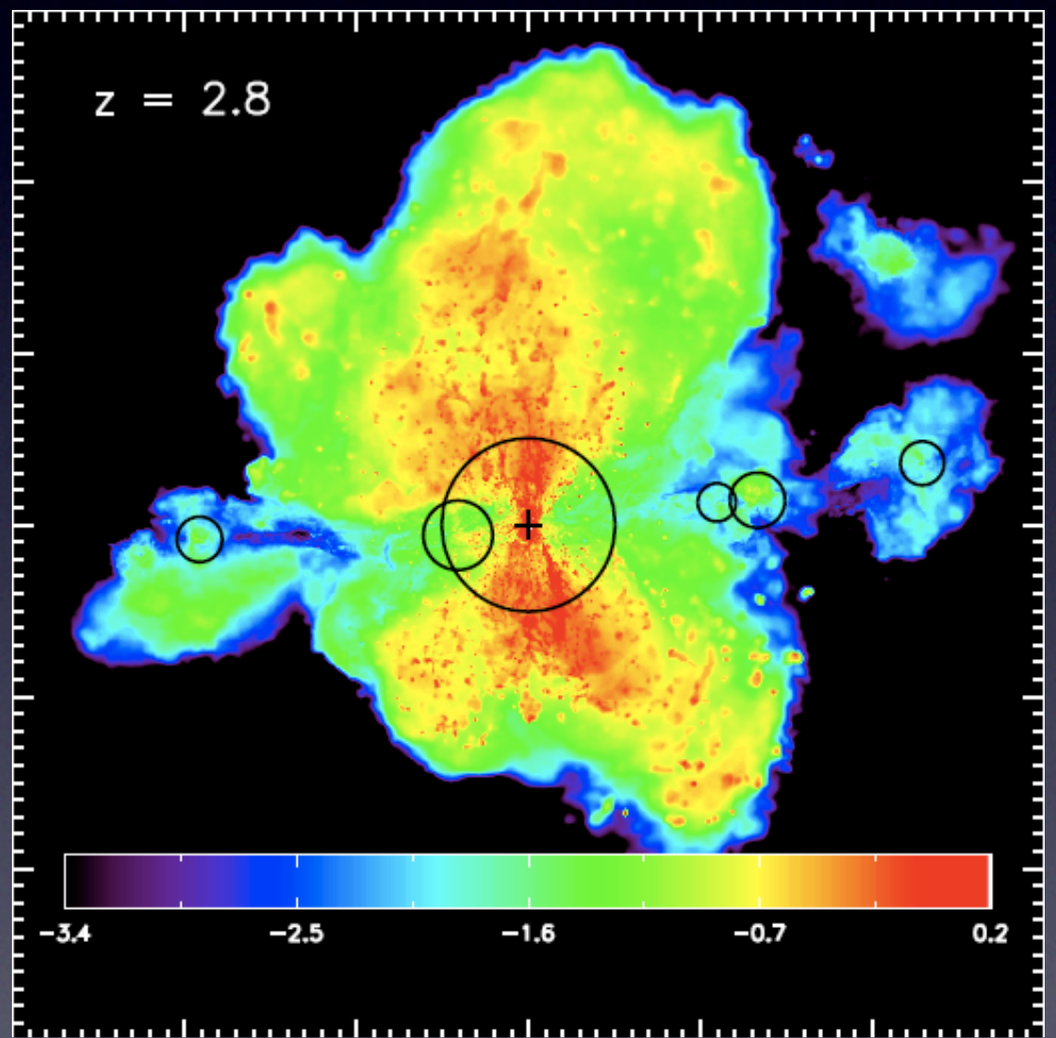

600 x 600 x 600 kpc3 projected map of gas metallicity. The disk is viewed nearly edge on

Kinematics of the Metal-Enriched CGM

- 600 x 600 x 10 kpc slice, projected to x-y plane, disk nearly edge-on
- Max projected averaged velocity ~300 km/s (host)
- Metallicity is high along the miner axis but non-zero along the major axis (Kacprzak+2012)
- Average outflow velocity decrease at larger distances and join the inflow -- halo fountain (Oppenheimer+ 2010)

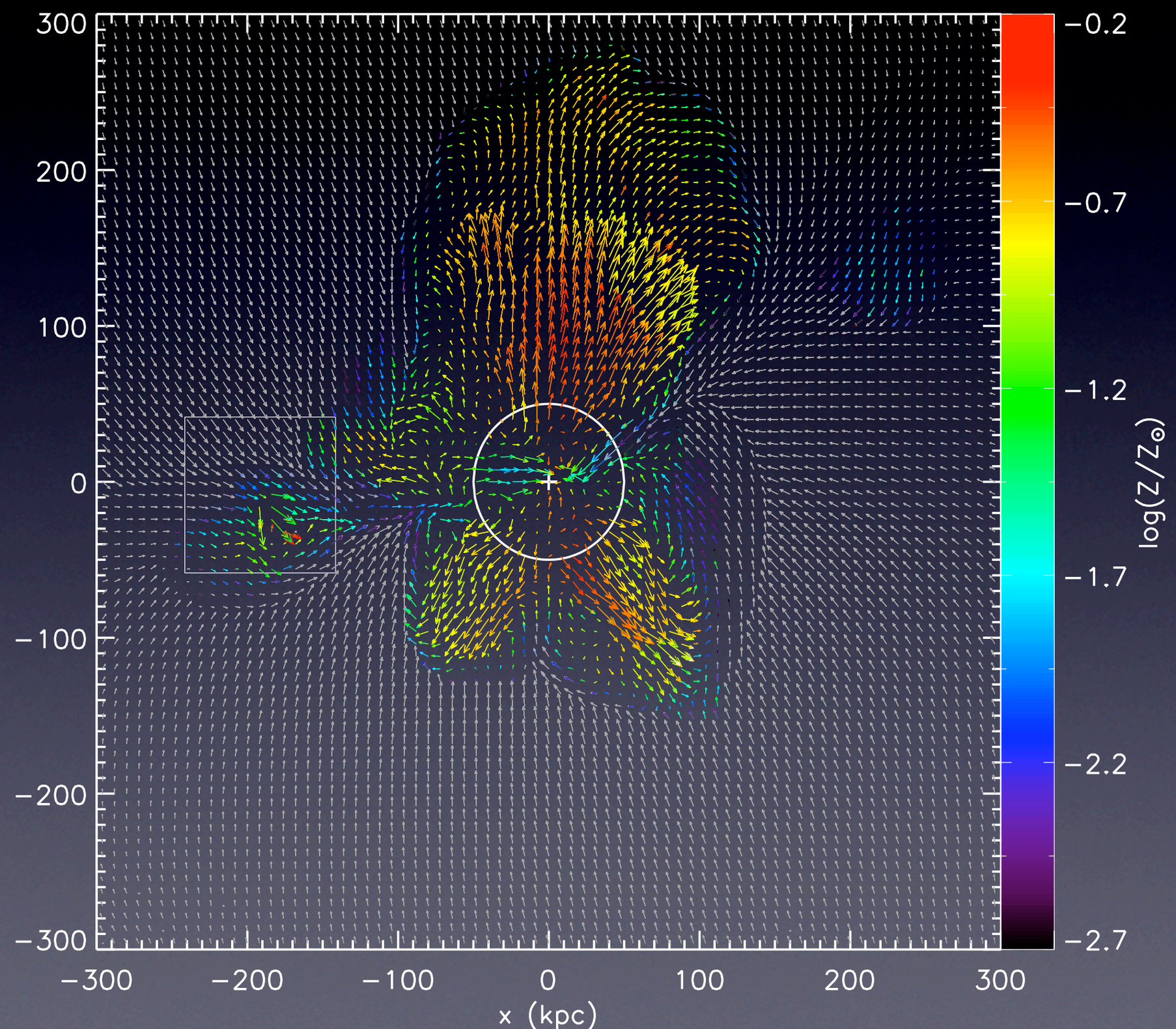

Kinematics of the Metal-Enriched CGM

- 600 x 600 x 10 kpc slice, projected to x-y plane, disk nearly edge-on
- Max projected averaged velocity ~300 km/s (host)
- Metallicity is high along the miner axis but non-zero along the major axis (Kacprzak+2012)
- Average outflow velocity decrease at larger distances and join the inflow -- halo fountain (Oppenheimer+ 2010)

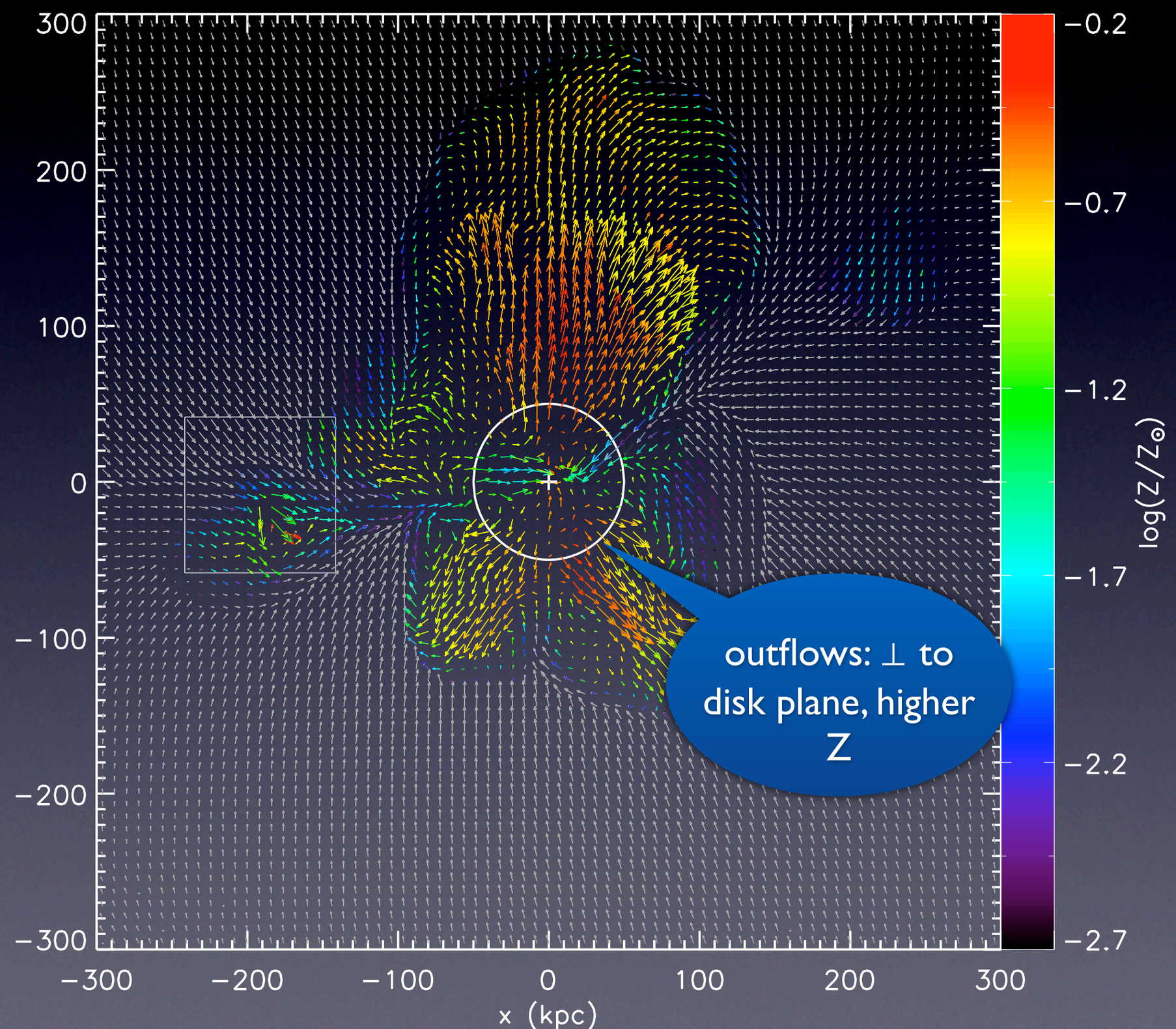

Kinematics of the Metal-Enriched CGM

- 600 x 600 x 10 kpc slice, projected to x-y plane, disk nearly edge-on
- Max projected averaged velocity ~300 km/s (host)
- Metallicity is high along the miner axis but non-zero along the major axis (Kacprzak+2012)
- Average outflow velocity decrease at larger distances and join the inflow -- halo fountain (Oppenheimer+ 2010)

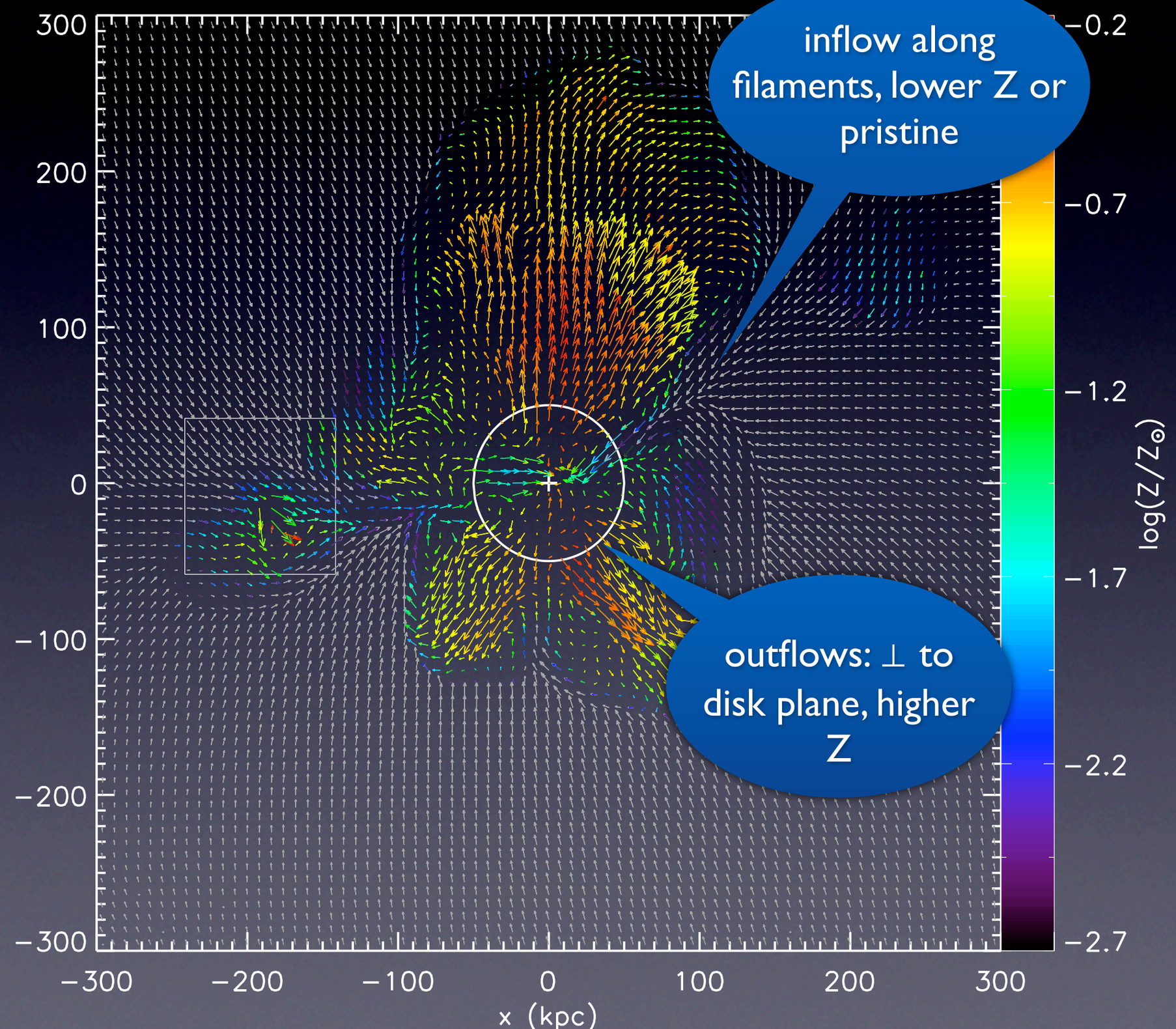

Kinematics of the Metal-Enriched CGM

- 600 x 600 x 10 kpc slice, projected to x-y plane, disk nearly edge-on
- Max projected averaged velocity ~300 km/s (host)
- Metallicity is high along the miner axis but non-zero along the major axis (Kacprzak+2012)
- Average outflow velocity decrease at larger distances and join the inflow -- halo fountain (Oppenheimer+ 2010)

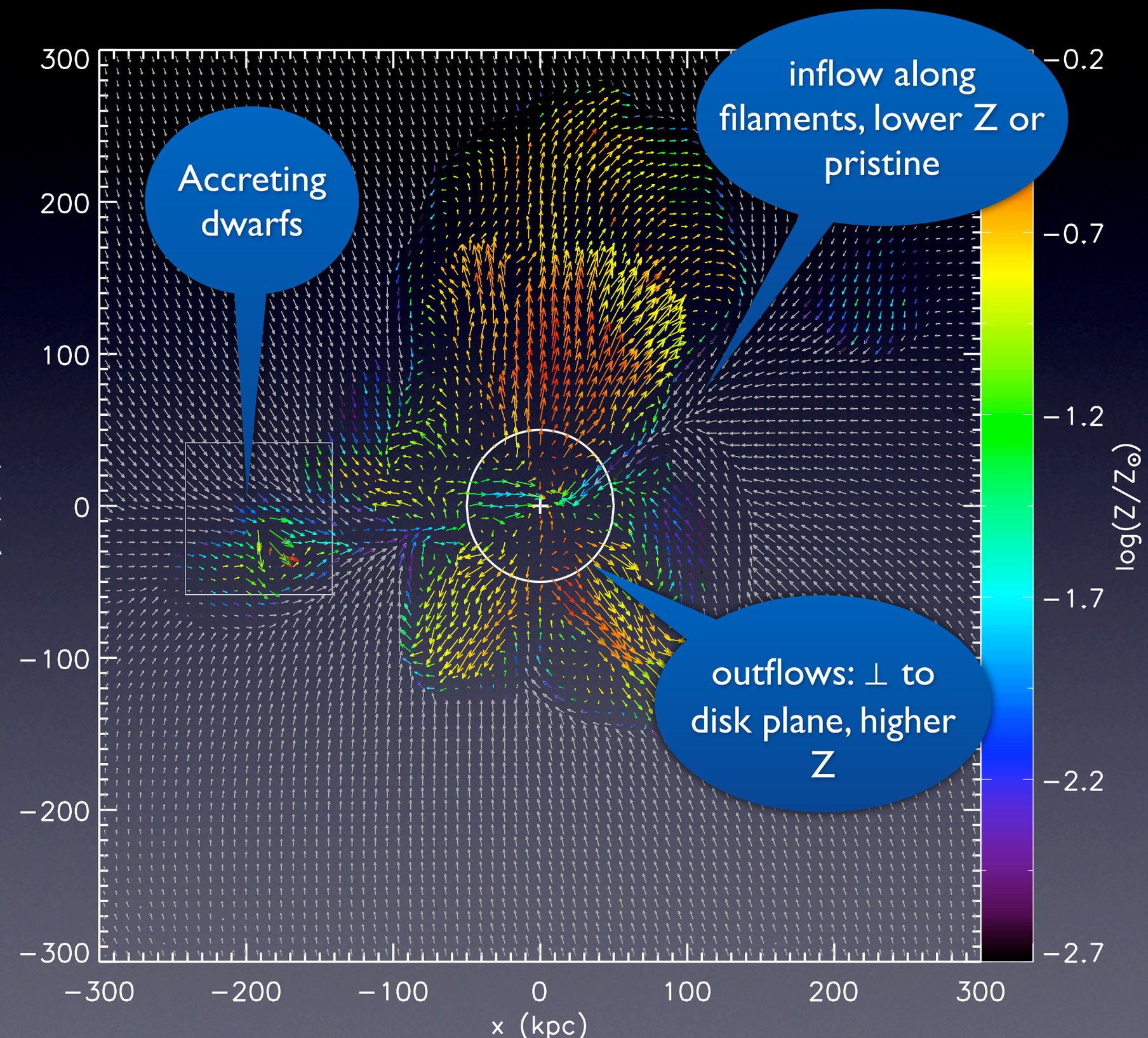

CGM Metals Traced by Different Ions

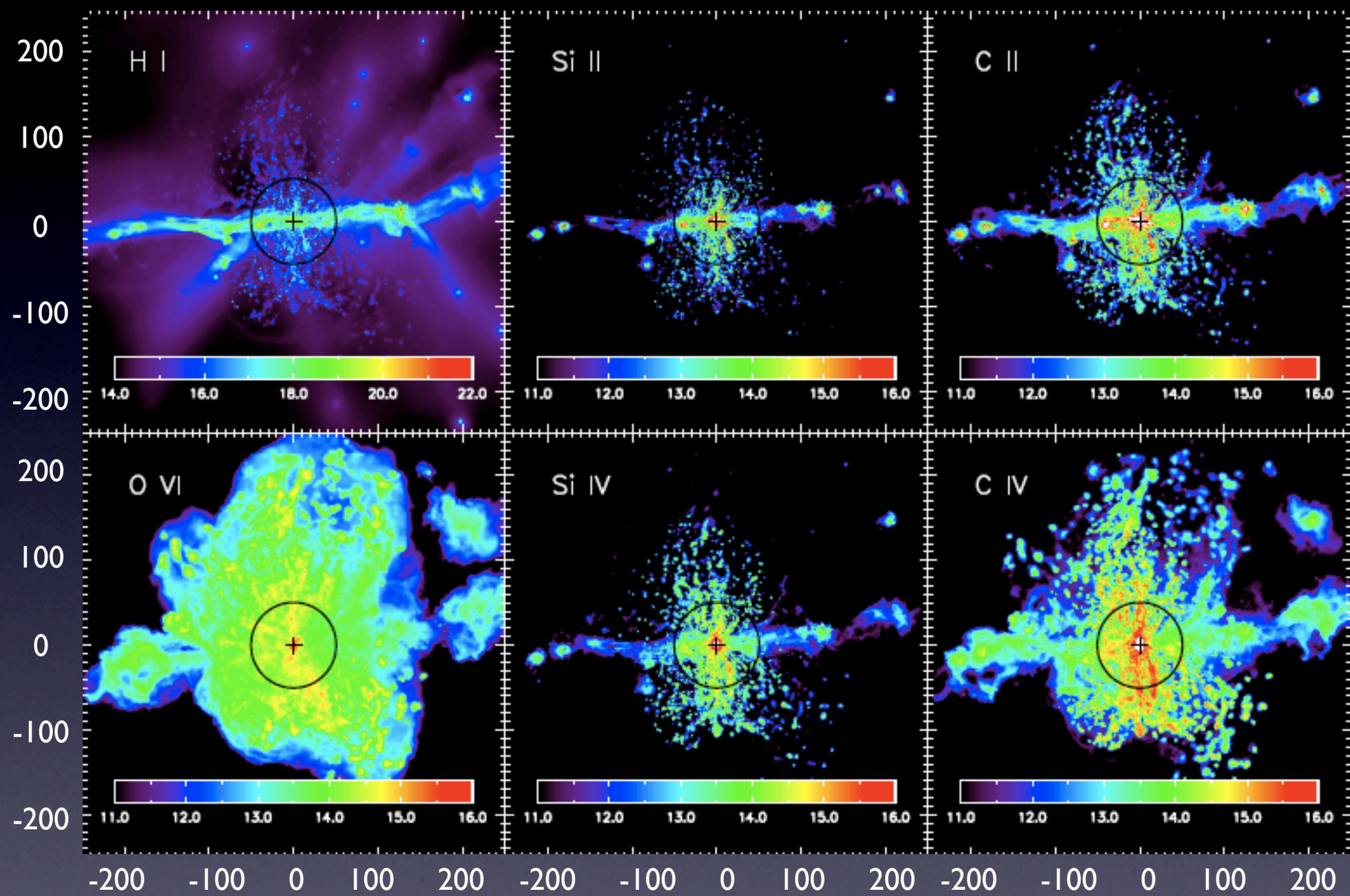

HI: 10^{14}-10^{21} cm^{-2}

Metals: 10^{11}-10^{16} cm^{-2}

Calculating ion fractions:

- UVB + non-uniform stellar UV assuming constant SFR 20 Msun/yr
- Photo-heating of local UV not included
- Assuming optically thin

- Multi-phase CGM: low and high ions co-exist in same absorbers
- Covering factors of low ions (C II, Si II) decrease more rapidly than high ions
- O VI has large covering factor up to 4 R_{vir}, M_O(CGM) ~5x 10^7 M_{sun}> M_O(ISM)

High ions: Collisional Ionization or Photoionization?

Cooler (T~3-5 $\times 10^4$ K), clumpier, photoionized OVI

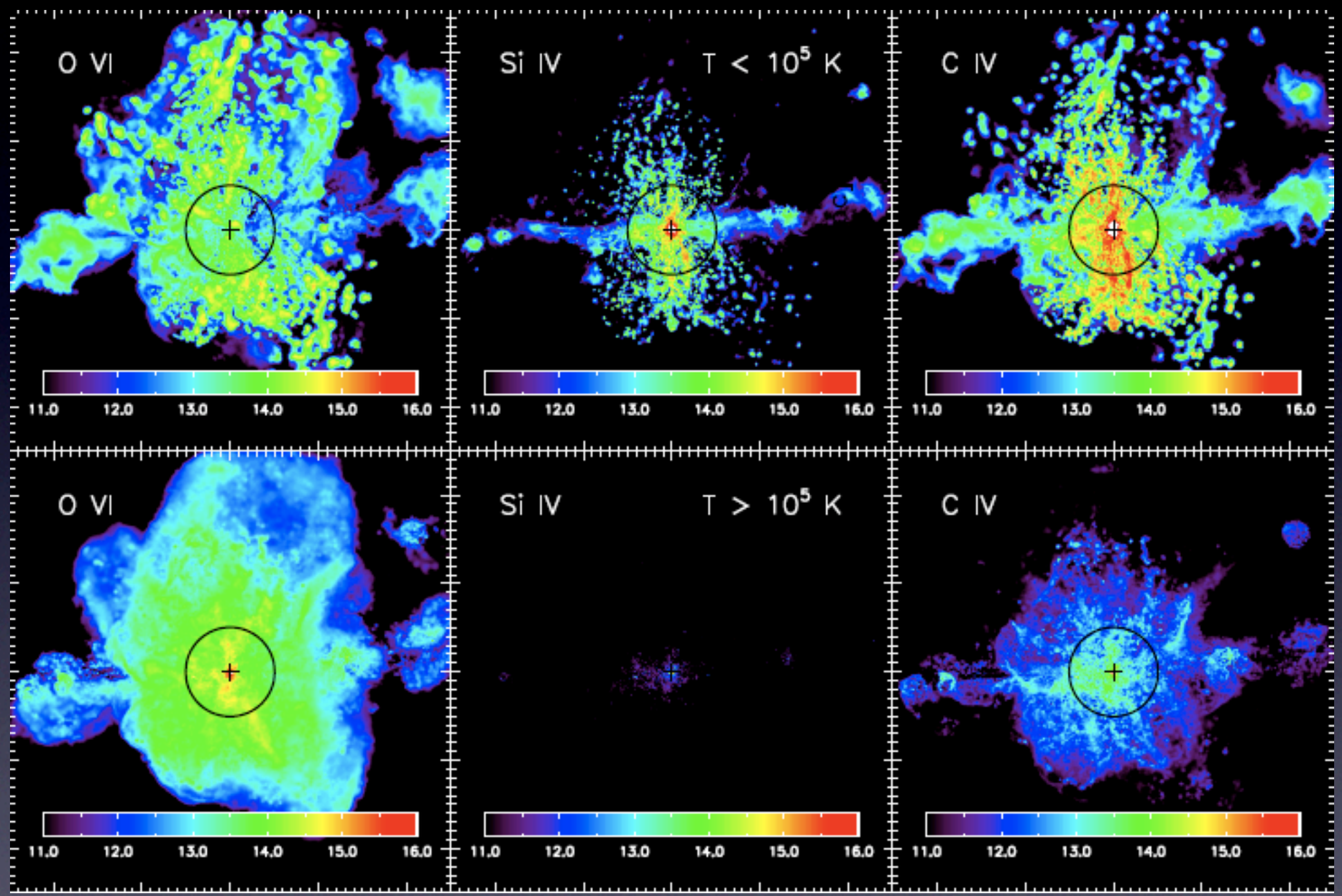

Si IV and C IV: Mostly photo-ionized

Hotter (T>10^5K), more diffuse, collisionally ionized OVI

- O VI: mostly collisional ionized within 2 Rvir, but photo-ionized at larger distance

Inflowing and Outflowing CGM

- Coexistence of inflow and outflow in the CGM:

- H I: cold inflow perpetrates viral radius. with $2R_{vir}$, 90% system with $N_{HI} > 10^{17.2}$ cm^{s} (LLS) is inflowing.
- Outflow gas increases the H I covering factor at large b.
- Low ions (C II or Si II) similar to H I

- O VI: by mass 68% outflow, 32% inflow
- C IV & Si IV: inflow and outflow contribute similarly

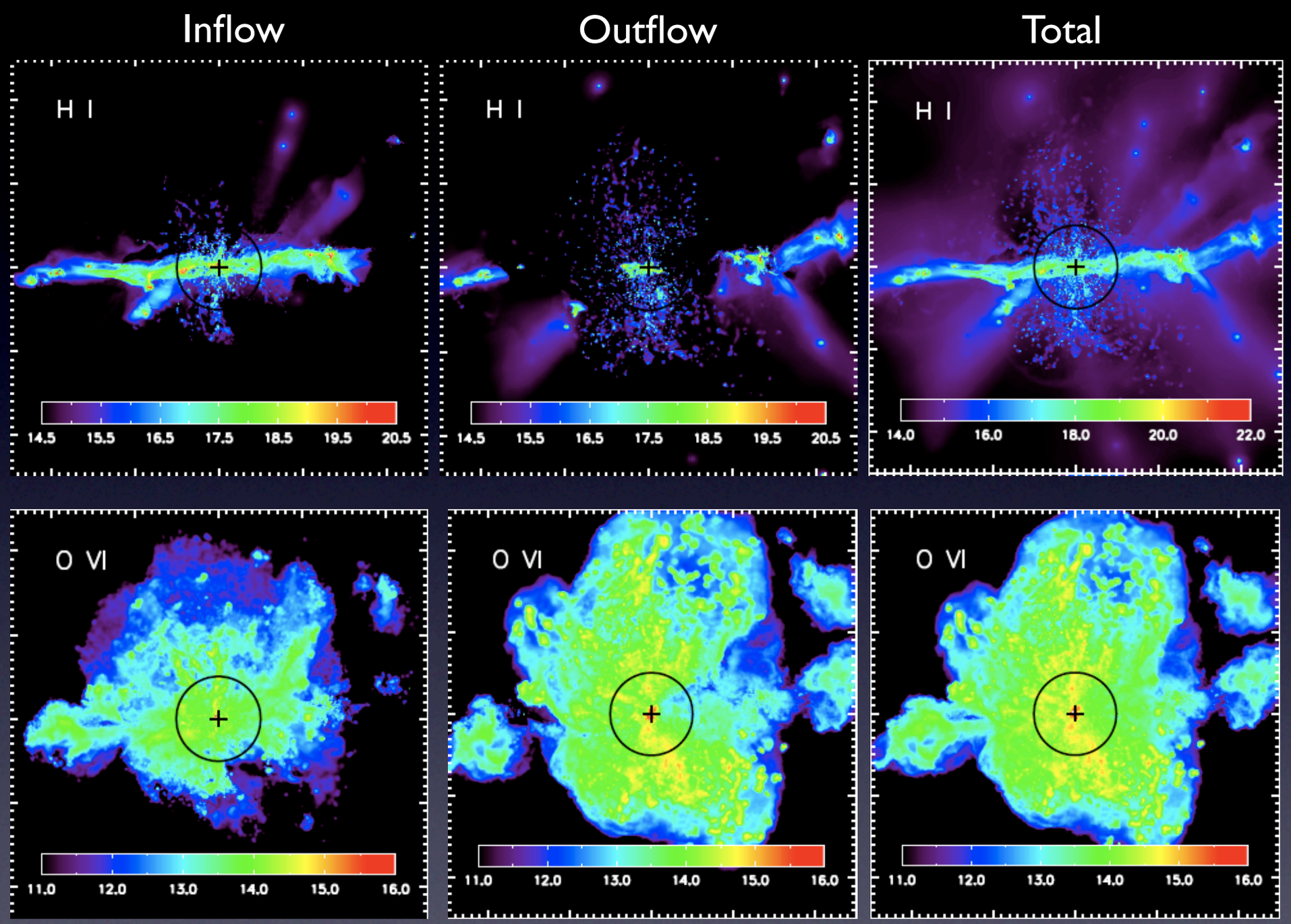

	H I	Si II	C II	Si IV	C IV	O VI
Inflow mass (%)	77%	66%	66%	50%	44%	32%

Synthetic Absorption Spectra

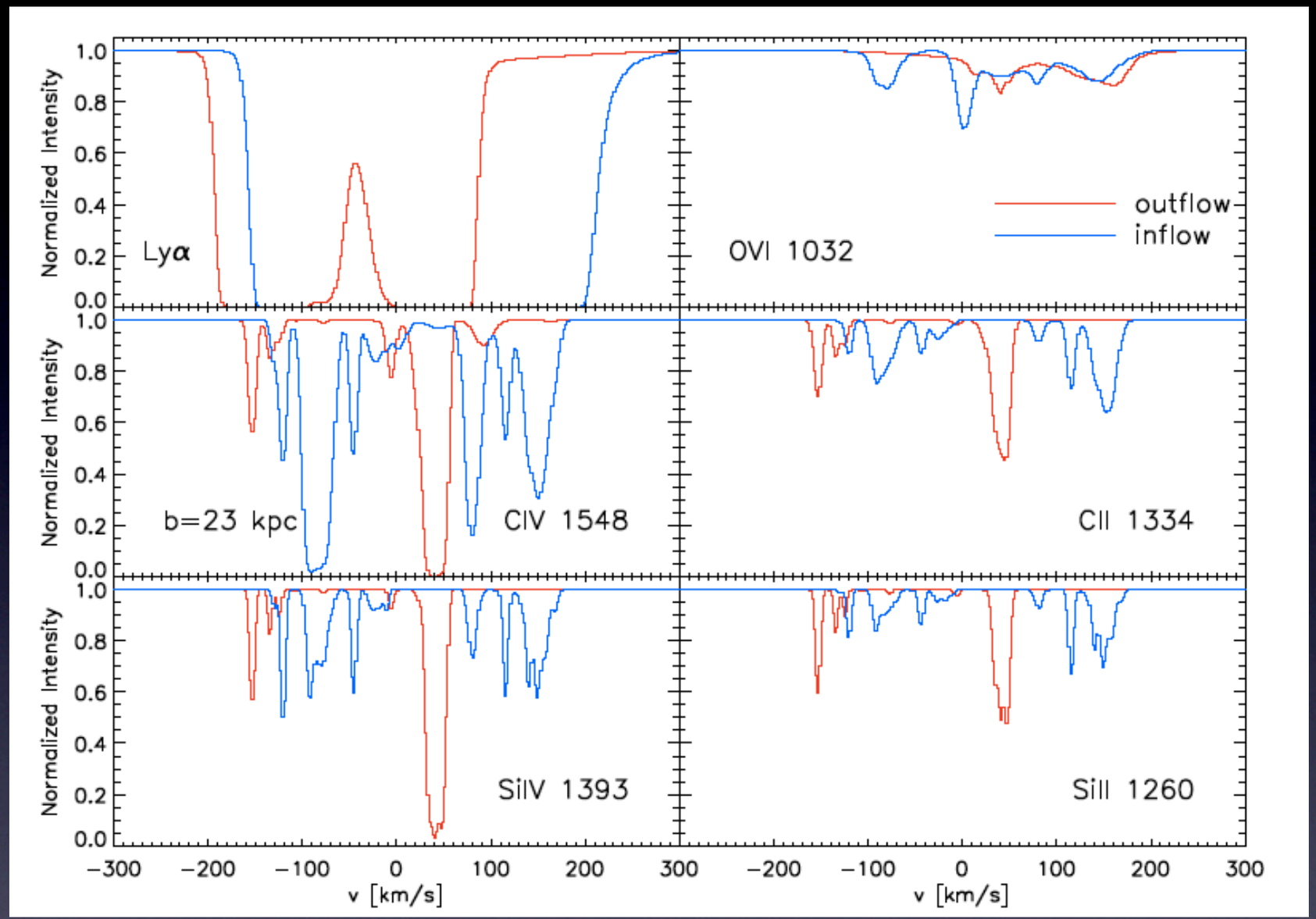

- Optical depth $\tau(\nu) = \sum_j (m_j Z_j/m) W_{2D}(r_{jl}, h_j) \sigma_j(\nu)$; $\sigma_j(\nu)$ - cross section (Voigt function), $W_{2D}(r_{jl}, h_j)$ - 2D SPH kernel

- Rest frame equivalent width: $W_0 = c/\nu_0^2 \int [1-e^{-\tau(\nu)}] d\nu$

Synthetic Absorption Spectra

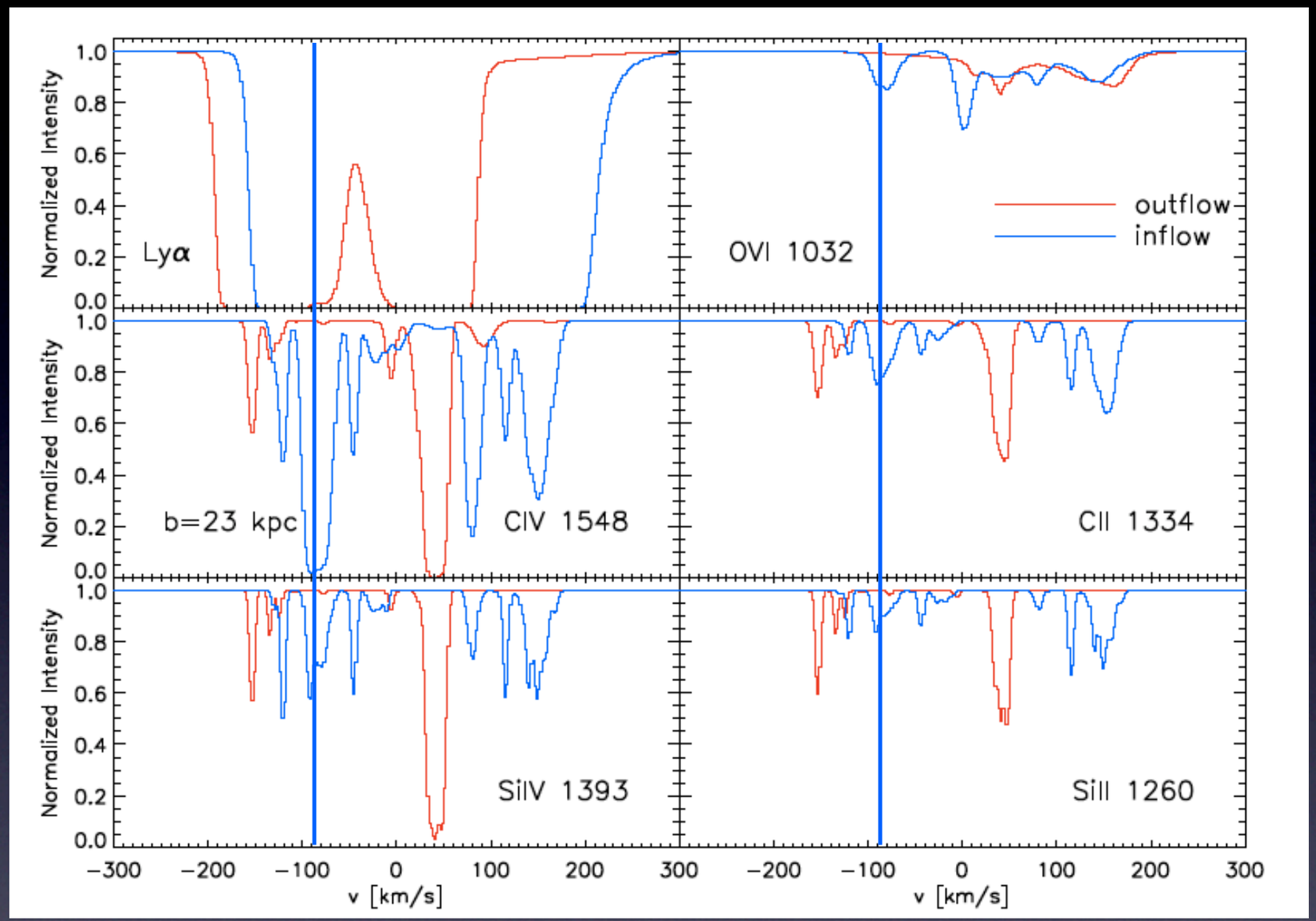

- Optical depth $\tau(\nu) = \sum_j (m_j Z_j/m) W_{2D}(r_{jl}, h_j)\sigma_j(\nu)$; $\sigma_j(\nu)$ - cross section (Voigt function), $W_{2D}(r_{jl}, h_j)$ - 2D SPH kernel

- Rest frame equivalent width: $W_0 = c/\nu_0^2 \int [1-e^{-\tau(\nu)}]d\nu$

Synthetic Absorption Spectra

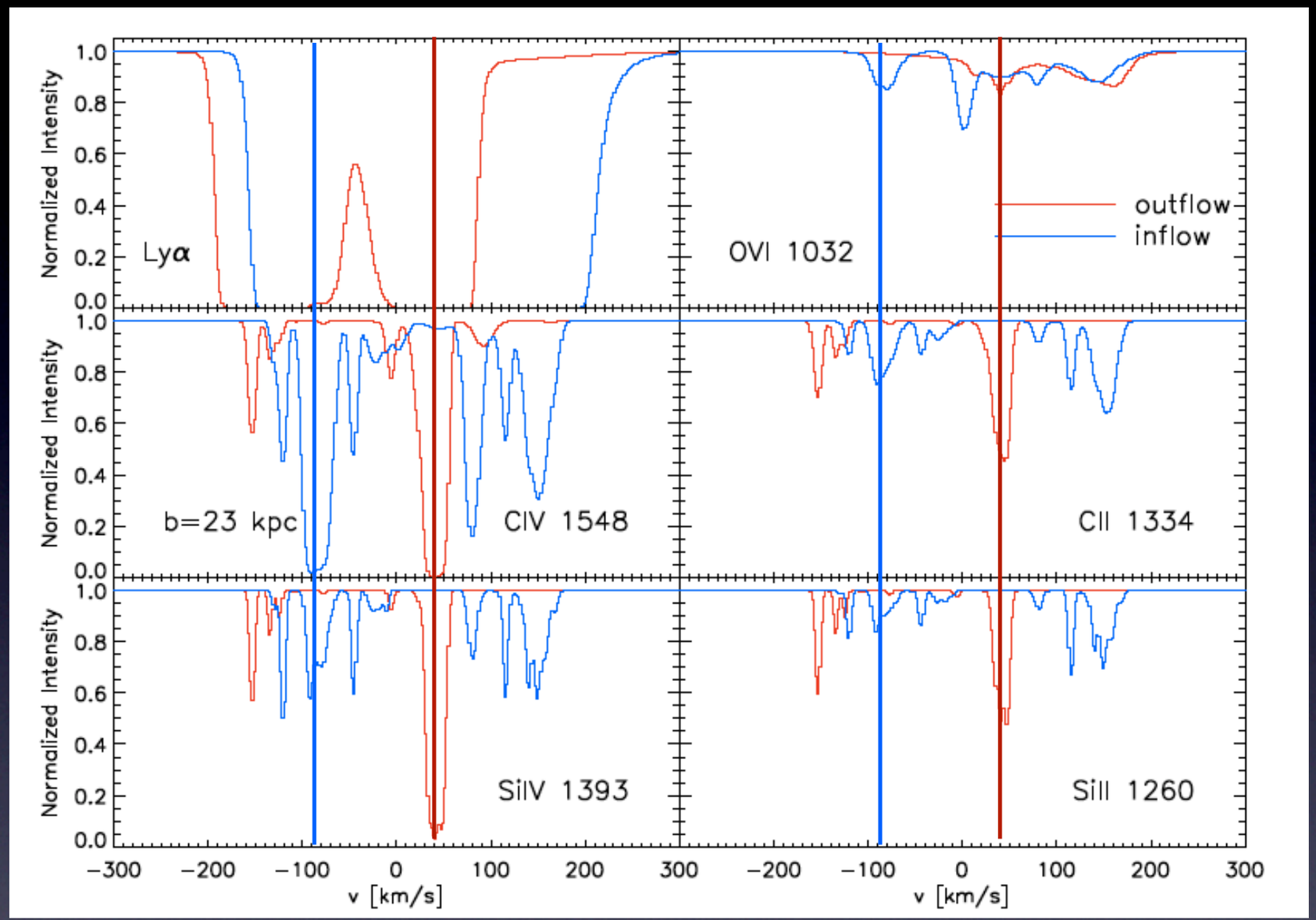

- Optical depth $\tau(\nu) = \sum_j (m_j Z_j/m) W_{2D}(r_{jl}, h_j)\sigma_j(\nu)$; $\sigma_j(\nu)$ - cross section (Voigt function), $W_{2D}(r_{jl}, h_j)$ - 2D SPH kernel

- Rest frame equivalent width: $W_0 = c/\nu_0^2 \int [1-e^{-\tau(\nu)}]d\nu$

Synthetic Absorption Spectra

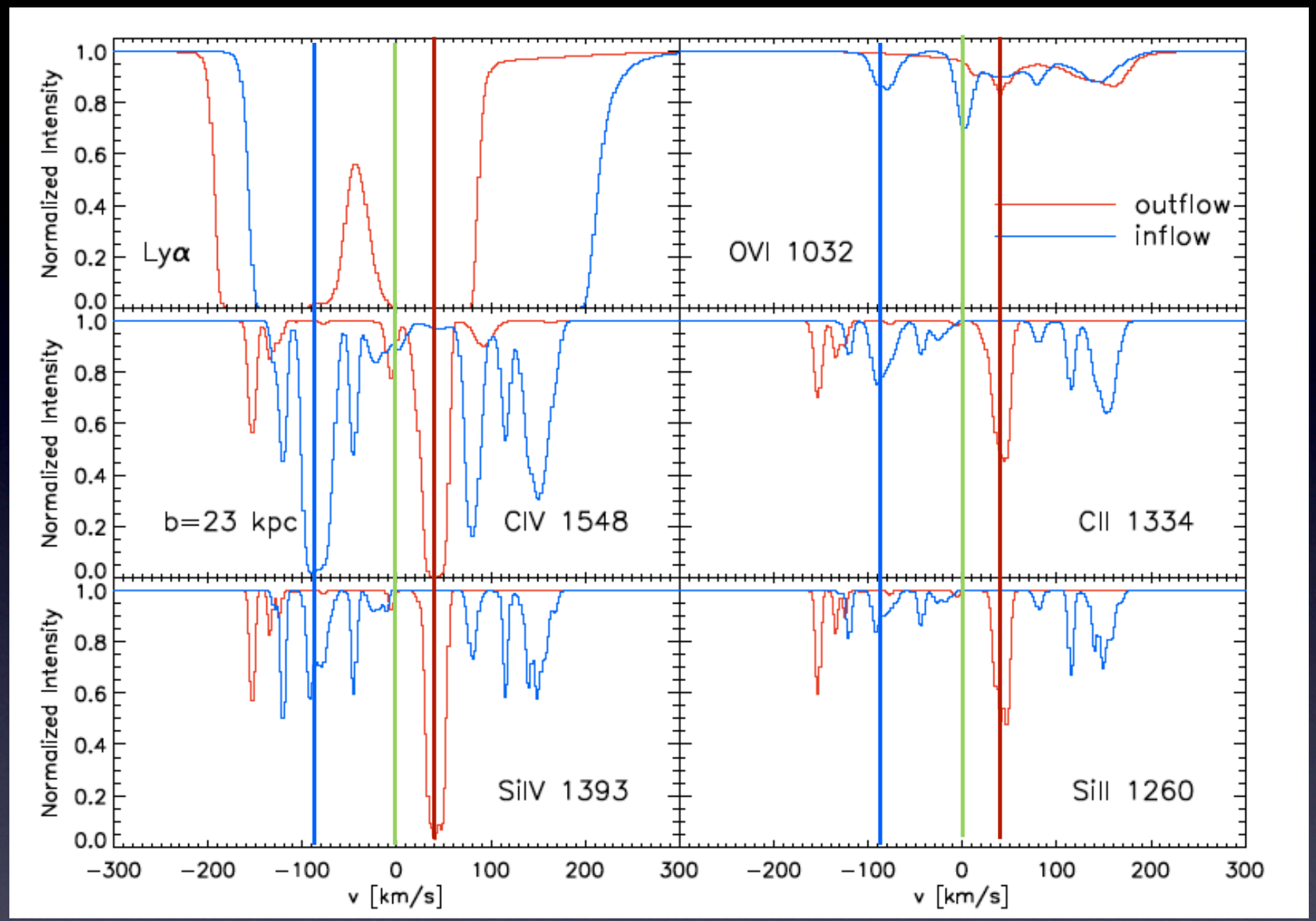

- Most, but not all, components exist in both high and low ions -- Multi-phase nature of absorbers

- Optical depth $\tau(\nu) = \sum_j (m_j Z_j/m) W_{2D}(r_{jl}, h_j) \sigma_j(\nu)$; $\sigma_j(\nu)$ - cross section (Voigt function), $W_{2D}(r_{jl}, h_j)$ - 2D SPH kernel

- Rest frame equivalent width: $W_0 = c/\nu_0^2 \int [1-e^{-\tau(\nu)}] d\nu$

Synthetic Absorption Spectra

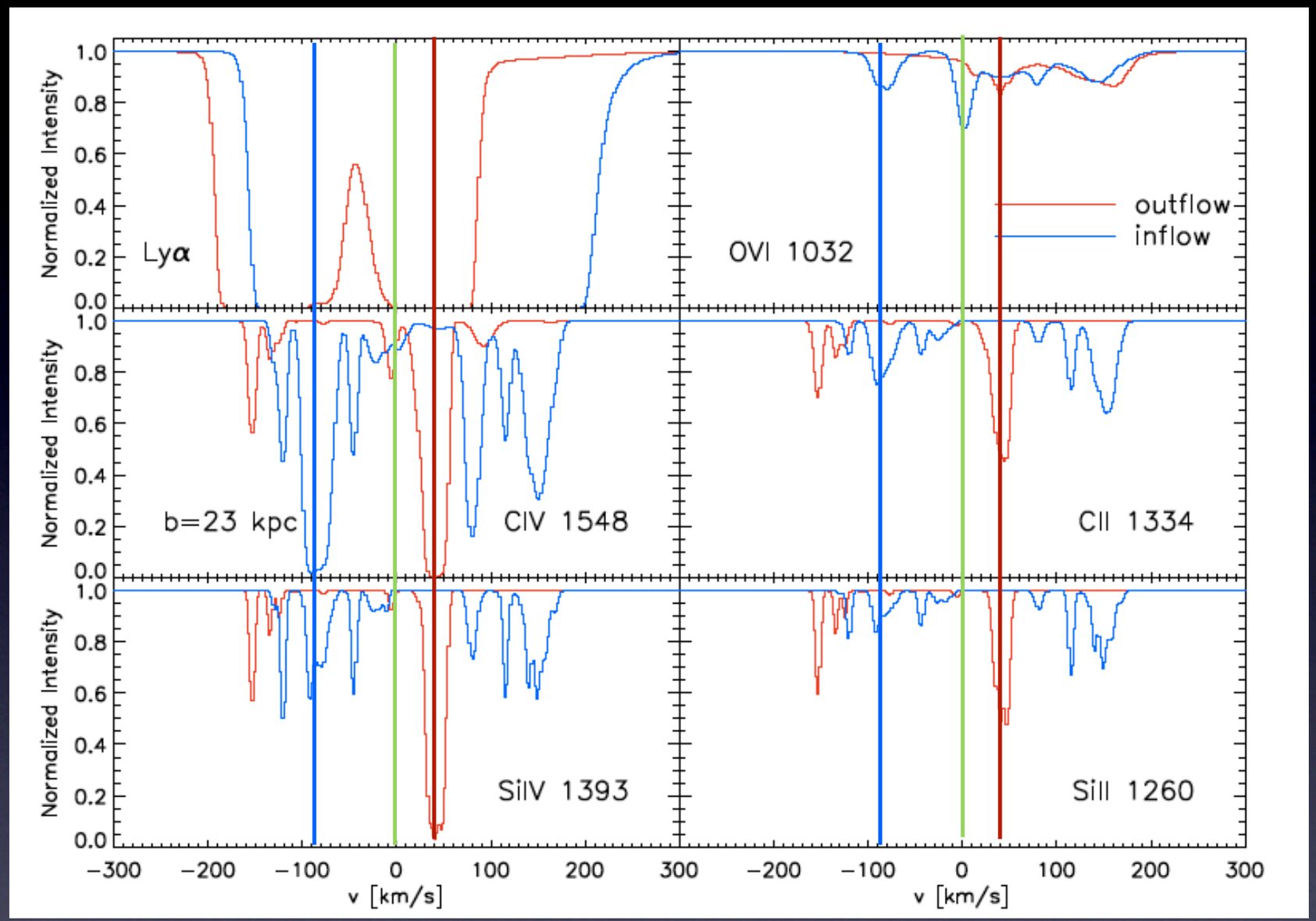

- Most, but not all, components exist in both high and low ions -- Multi-phase nature of absorbers
- Velocity range ~ ± 300 km/s

- Optical depth $\tau(\nu) = \sum_j (m_j Z_j/m) W_{2D}(r_{jl}, h_j) \sigma_j(\nu)$; $\sigma_j(\nu)$ - cross section (Voigt function), $W_{2D}(r_{jl}, h_j)$ - 2D SPH kernel

- Rest frame equivalent width: $W_0 = c/\nu_0^2 \int [1-e^{-\tau(\nu)}] d\nu$

Synthetic Absorption Spectra

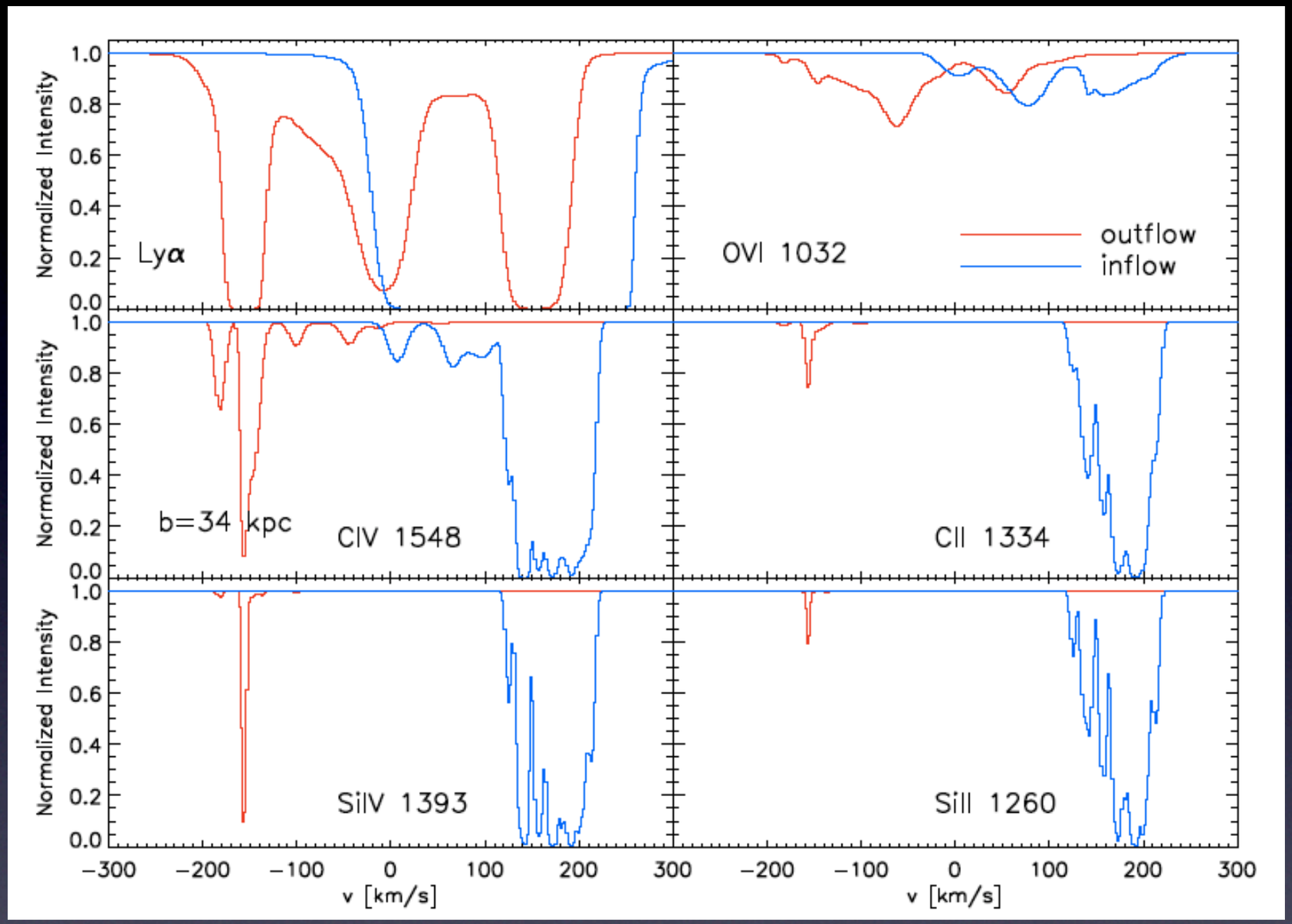

- Most, but not all, components exist in both high and low ions -- Multi-phase nature of absorbers
- Velocity range ~ ± 300 km/s

- Optical depth $\tau(\nu) = \sum_j (m_j Z_j/m) W_{2D}(r_{jl}, h_j) \sigma_j(\nu)$; $\sigma_j(\nu)$ - cross section (Voigt function), $W_{2D}(r_{jl}, h_j)$ - 2D SPH kernel

- Rest frame equivalent width: $W_0 = c/\nu_0^2 \int [1-e^{-\tau(\nu)}] d\nu$

Synthetic Absorption Spectra

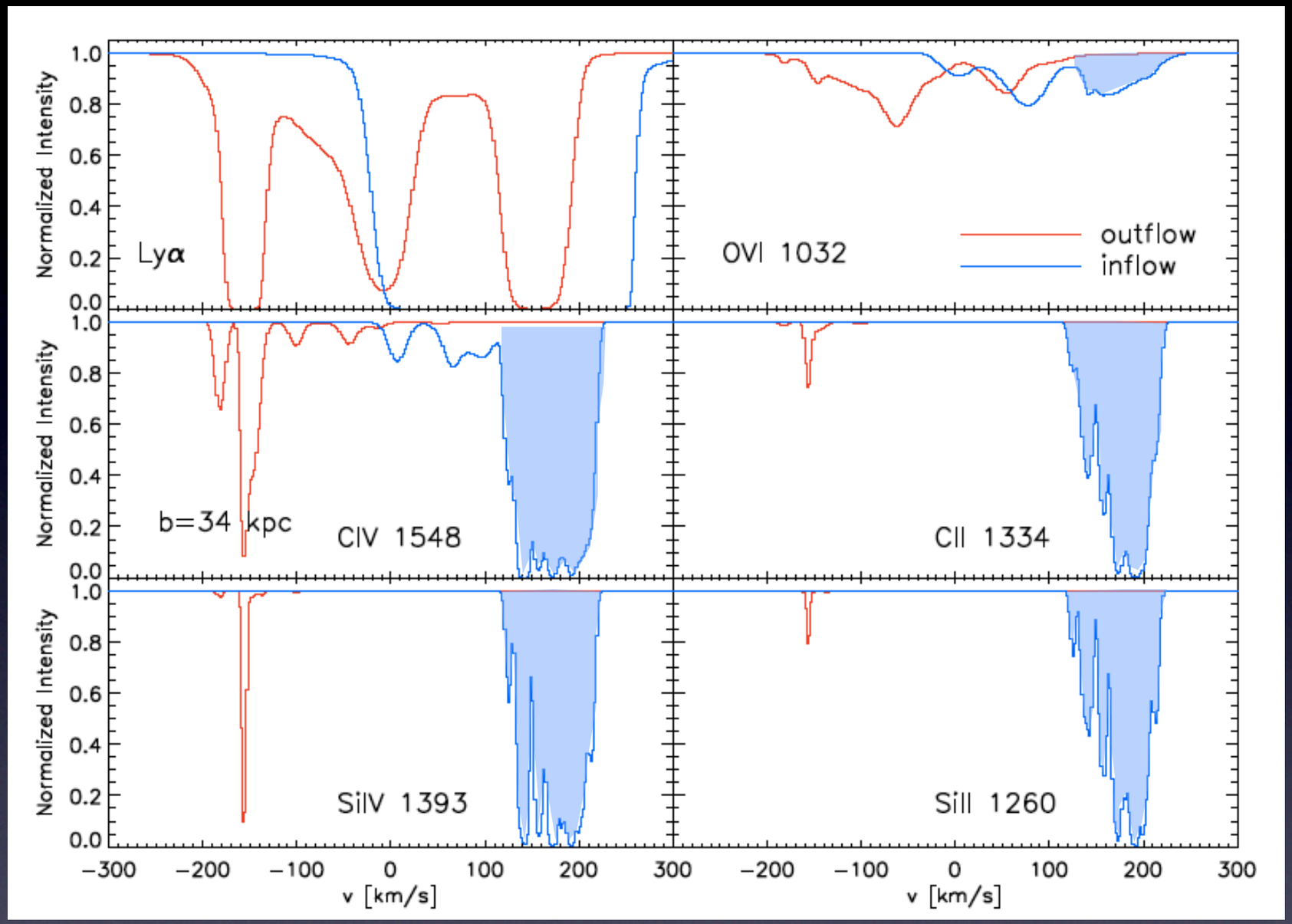

- Most, but not all, components exist in both high and low ions -- Multi-phase nature of absorbers
- Velocity range ~ ± 300 km/s

- Metal enriched infalling gas:
- $R_{vir} < r < 2R_{vir}$
- $\delta \sim 100$
- $Z > 0.03\ Z_{sun}$
- Enriched gas around nearby dwarf galaxy

- Optical depth $\tau(\nu) = \sum_j (m_j Z_j/m) W_{2D}(r_{jl}, h_j)\sigma_j(\nu)$; $\sigma_j(\nu)$ - cross section (Voigt function), $W_{2D}(r_{jl}, h_j)$ - 2D SPH kernel

- Rest frame equivalent width: $W_0 = c/\nu_0^2 \int [1-e^{-\tau(\nu)}]d\nu$

W_0-b Relation and Comparison with Observations

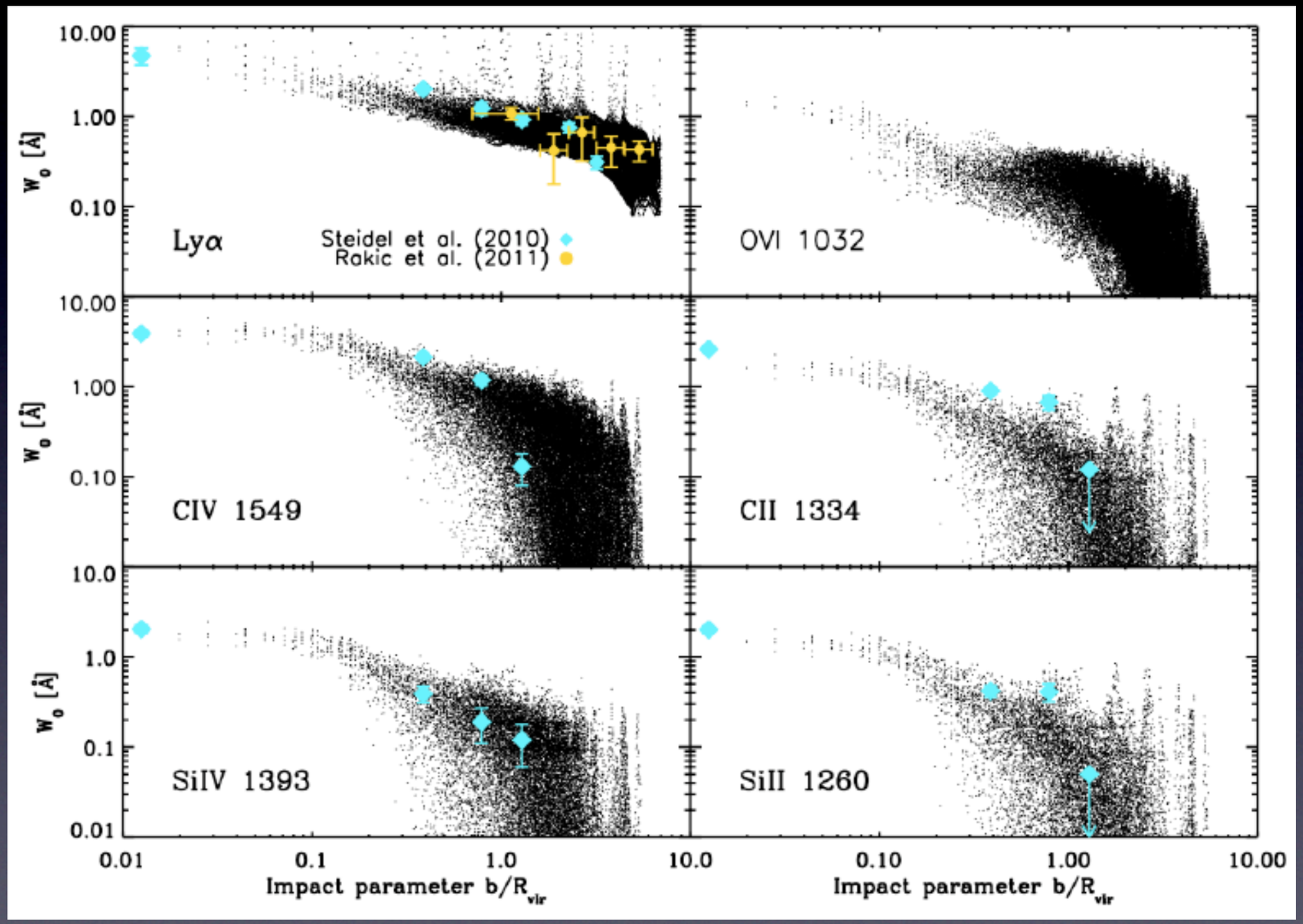

- Metal Line strength decline rapidly at 1-2 R_{vir}
- Line strength decline less fast for C IV, OVI and H I
- Ly α: remains strong to >~ 5 R_{vir}
- Broadly consistent with observations from Steidel+ (2010) and Rakic+ (2011)
- W_0 for metal ions: Higher than simulations without strong outflows (e.g., Fumagalli+ 2011)
- At small b, lines are mostly saturated -- W_0 determined by velocity

- 3 orthogonal projections, each has 500 x 500 evenly-spaced slightlines within b = 250 kpc region centered at the main host

W_0-b Relation and Comparison with Observations

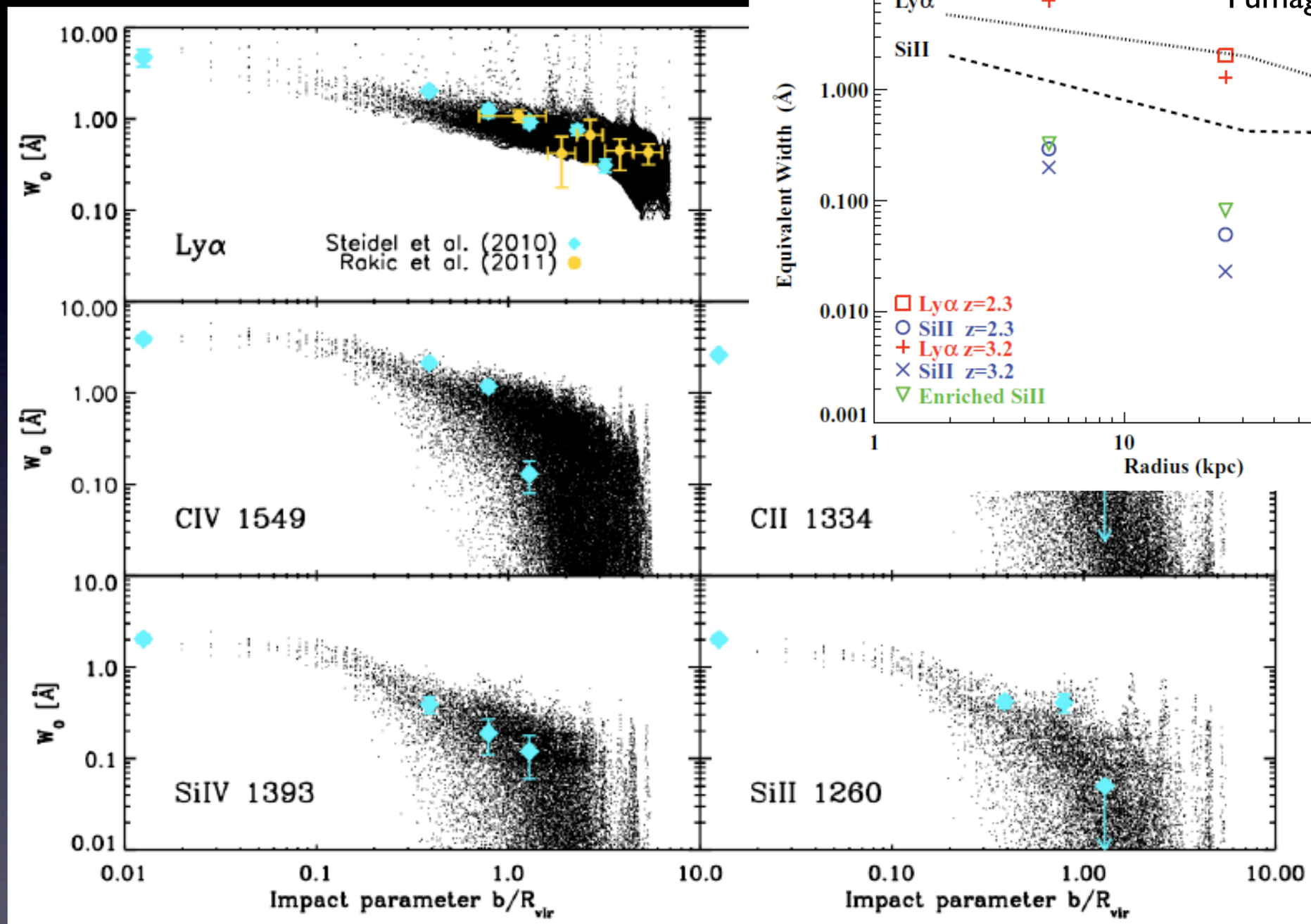

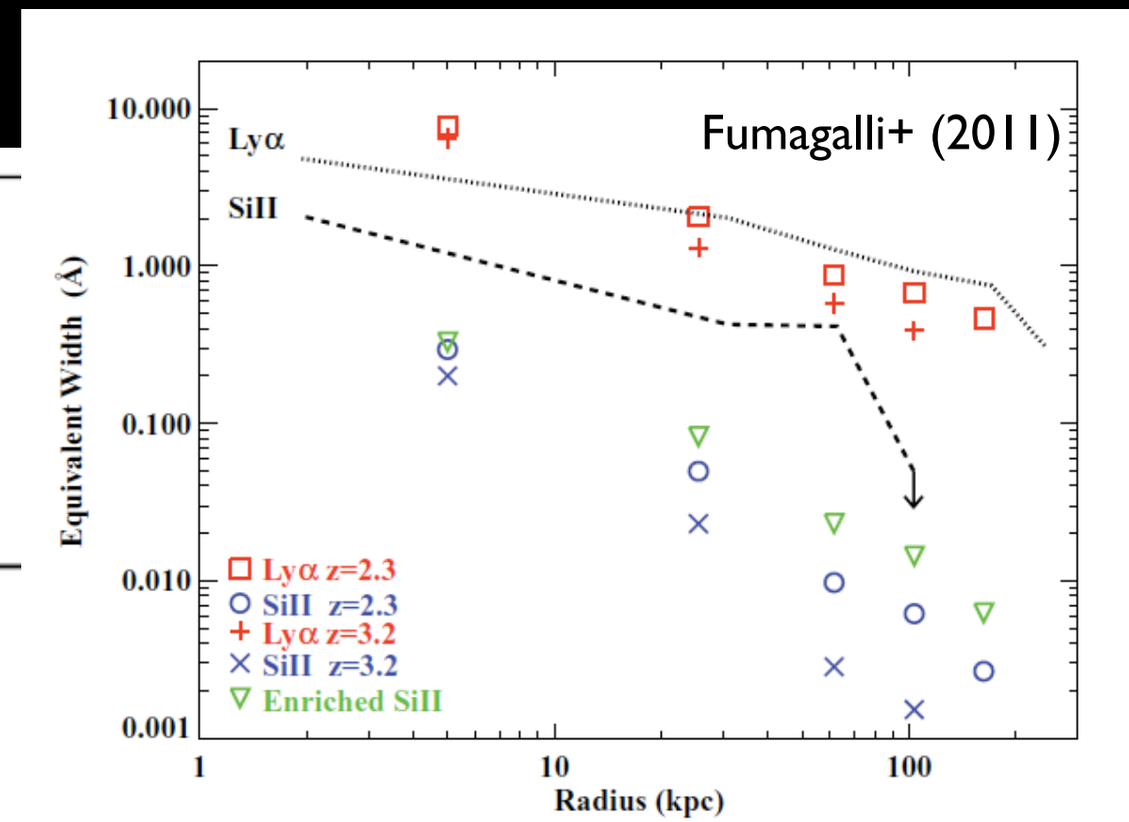

rength
ly at 1-2 R_{vir}

decline
C IV, OVI

s strong to

istent with
from
Steidel+ (2010) and
Rakic+ (2011)

- W_0 for metal ions: Higher than simulations without strong outflows (e.g., Fumagalli+ 2011)
- At small b, lines are mostly saturated -- W_0 determined by velocity

- 3 orthogonal projections, each has 500 x 500 evenly-spaced slightlines within b = 250 kpc region centered at the main host

Covering Factor of H I and Metal Ions

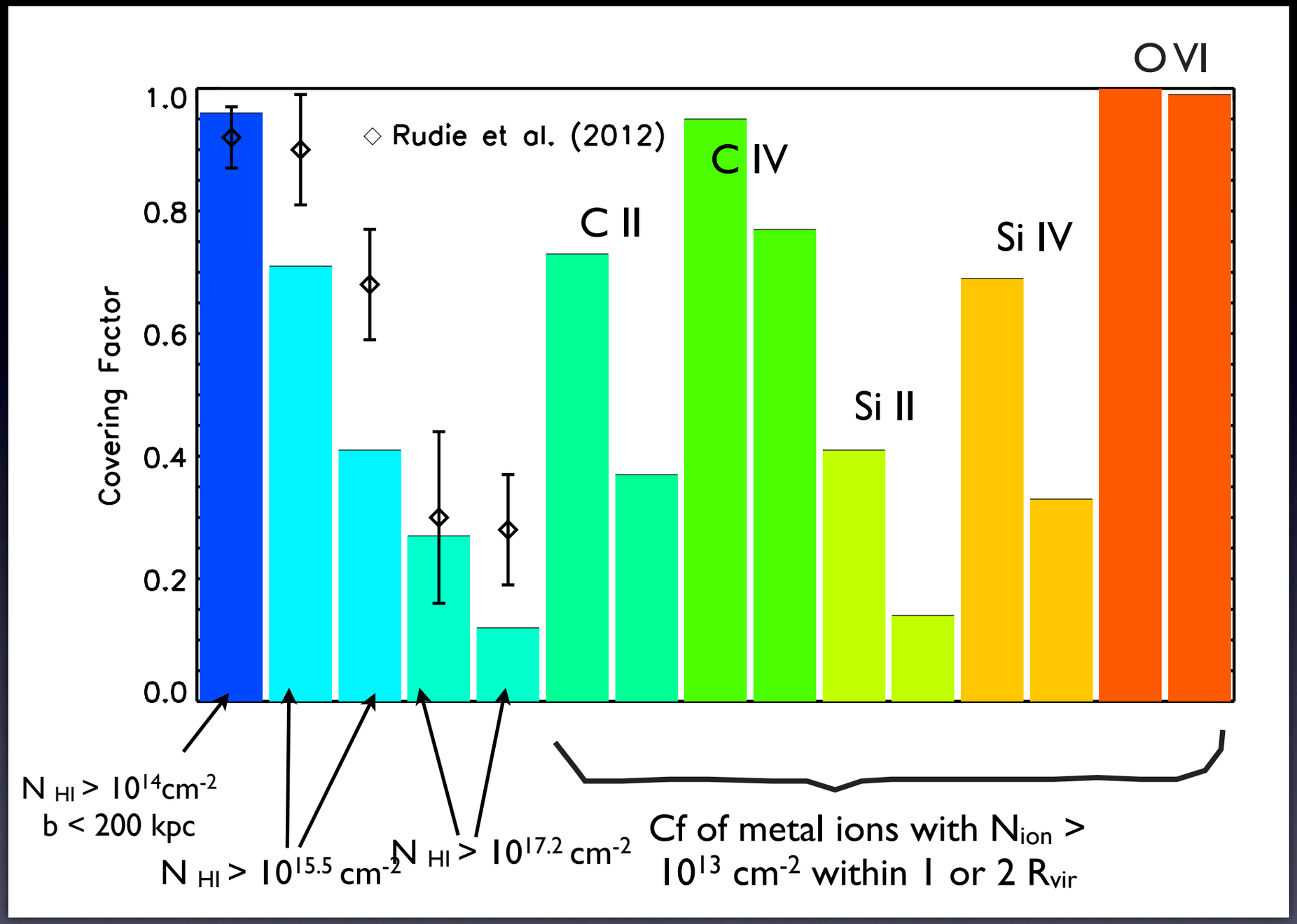

- O VI has covering factor (f_c) of unity in 2 $R_{vir.}$ C IV also have large f_c
- C II, Si II, Si IV: smaller f_c, decline fast when b > R_{vir}

- In reasonable agreement with Rudie+ (2012) for H I, but in the low side
- HI covering factor: slightly higher, but comparable to simulations without strong outflows (e.g. Fumagalli+2011, Faucher-Giguère & Kereš 2011)

Detecting the Cold Streams: H I and Low Ions

- Cold ($T < 10^5$ K) inflow rates at R_{vir} $dM_{in,\,cold}/dt = 18\ M_{sun}/yr$, comparable to the SFR; $M_{in,\,hot}/dt \sim 5M_{sun}/yr$
- 35% inflow gas from nearby dwarfs
- Within 2 Rvir: 90% of LLS are inflowing gas, $v_{in} <\sim 150$ -200 km/s

Detecting the Cold Streams: H I and Low Ions

Inflow only, optically thick gas

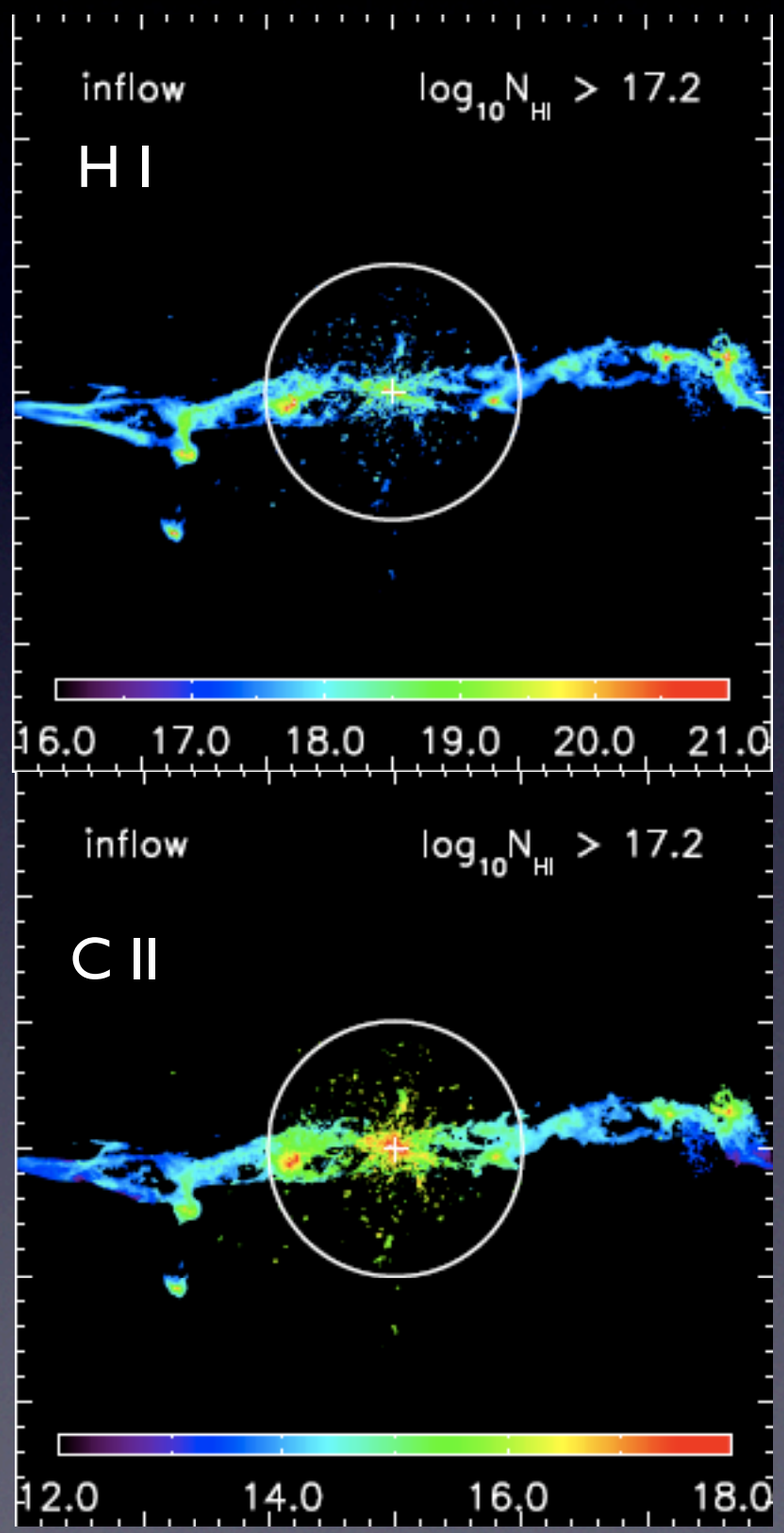

- Cold ($T < 10^5$ K) inflow rates at R_{vir} $dM_{in,\,cold}/dt = 18\ M_{sun}/yr$, comparable to the SFR; $M_{in,\,hot}/dt \sim 5 M_{sun}/yr$
- 35% inflow gas from nearby dwarfs
- Within 2 Rvir: 90% of LLS are inflowing gas, $v_{in} <\sim 150$ -200 km/s

Detecting the Cold Streams: H I and Low Ions

Inflow only, optically thick gas

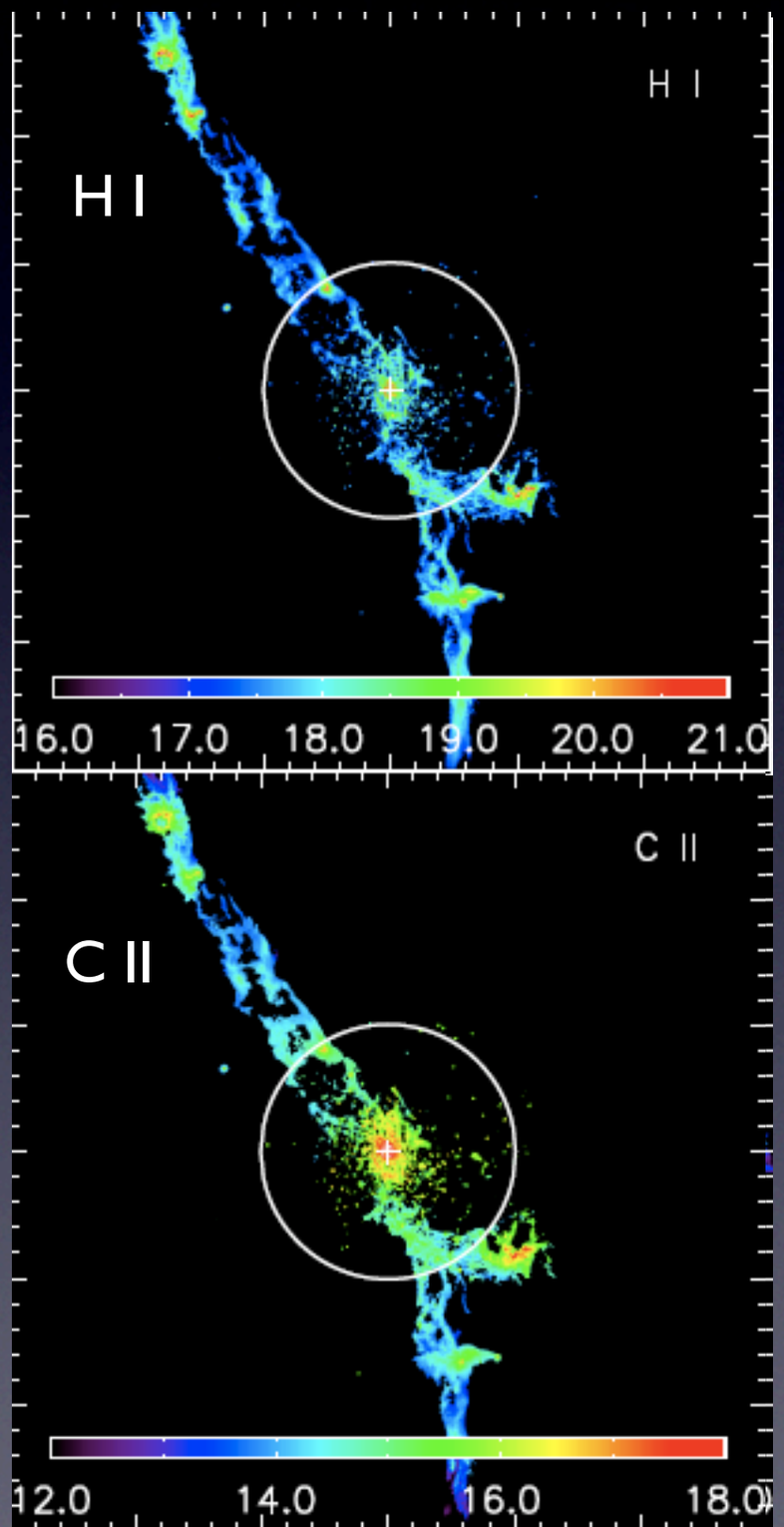

- Cold ($T < 10^5$ K) inflow rates at R_{vir} $dM_{in,\,cold}/dt = 18\ M_{sun}/yr$, comparable to the SFR; $M_{in,\,hot}/dt \sim 5 M_{sun}/yr$
- 35% inflow gas from nearby dwarfs
- Within 2 Rvir: 90% of LLS are inflowing gas, $v_{in} <\sim 150$ -200 km/s

Detecting the Cold Streams: H I and Low Ions

Inflow only, optically thick gas

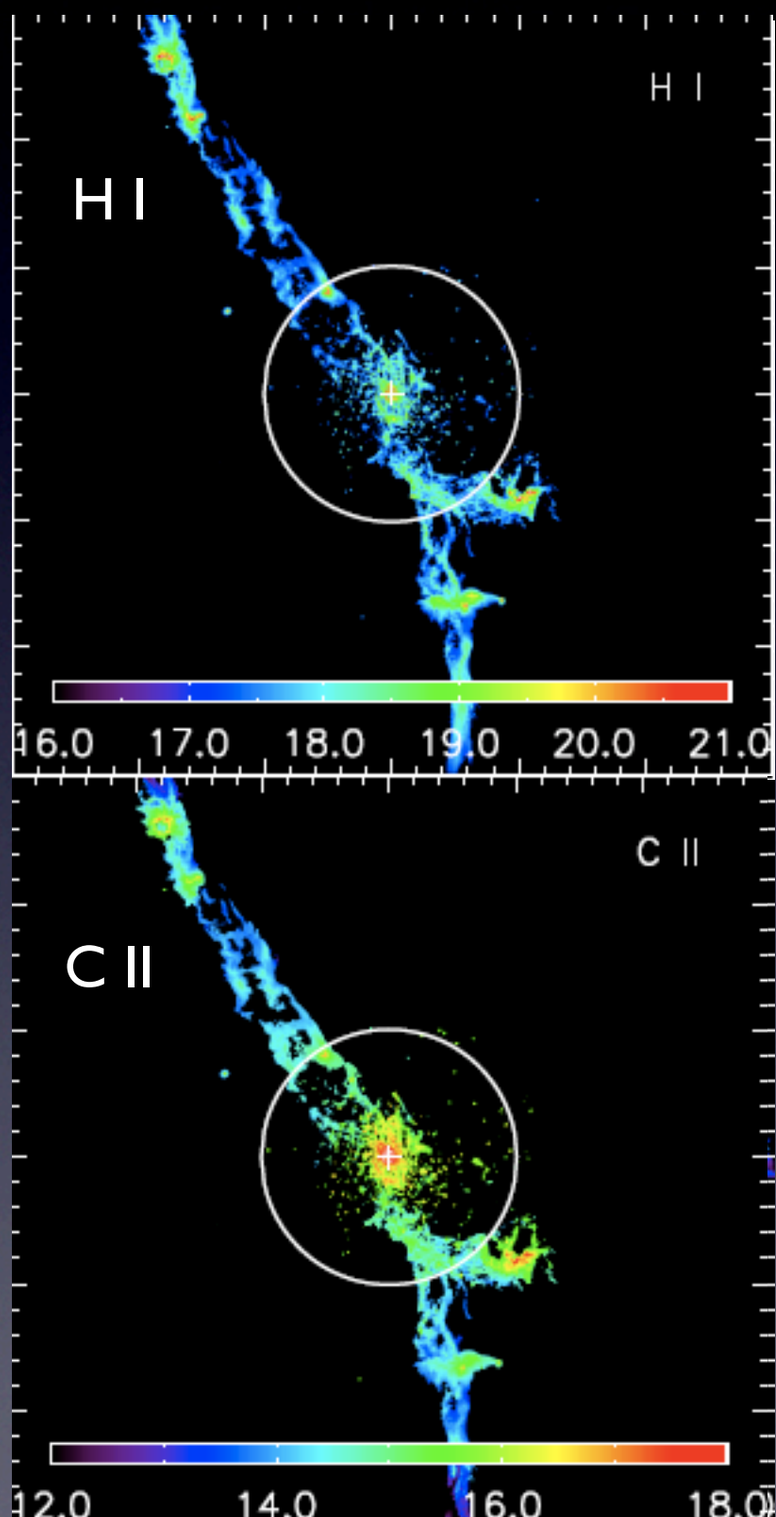

- Cold ($T < 10^5$ K) inflow rates at R_{vir} $dM_{in,\,cold}/dt = 18\ M_{sun}/yr$, comparable to the SFR; $M_{in,\,hot}/dt \sim 5 M_{sun}/yr$
- 35% inflow gas from nearby dwarfs
- Within 2 Rvir: 90% of LLS are inflowing gas, $v_{in} <\sim 150$ -200 km/s
- Cold inflows are enriched: $Z_{LLS} > 0.03\ Z_{sun}$ for $r < R_{vir}$, and $Z_{LLS} > 0.01\ Z_{sun}$ within $2R_{vir}$
- Still lower than outflow metallicities $Z_{out} = 0.1\text{-}0.5\ Z_{sun}$

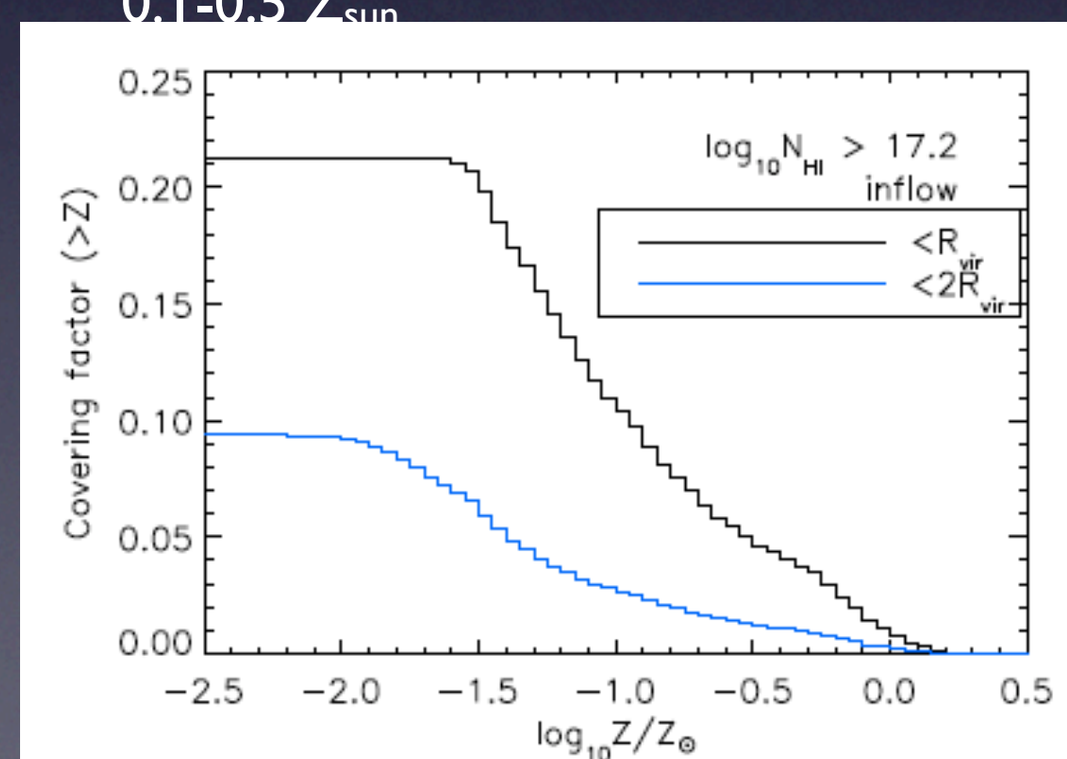

The N_{OVI}-b Relation in Eris2: Comparison with Low z Starburst Galaxies

- At z = 2.8, Eris2 has sSFR ~ 10^{-9} yr^{-1}, close to the local star burst galaxies in Tumlinson + (2011) and Prochaska+ (2011)
- N_{OVI}-b relation in good agreement with observations typical N_{OVI} >~10^{13-14} cm^{-2} up to 100 - 150 kpc
- N_{OVI} -b mostly determined by SFR?

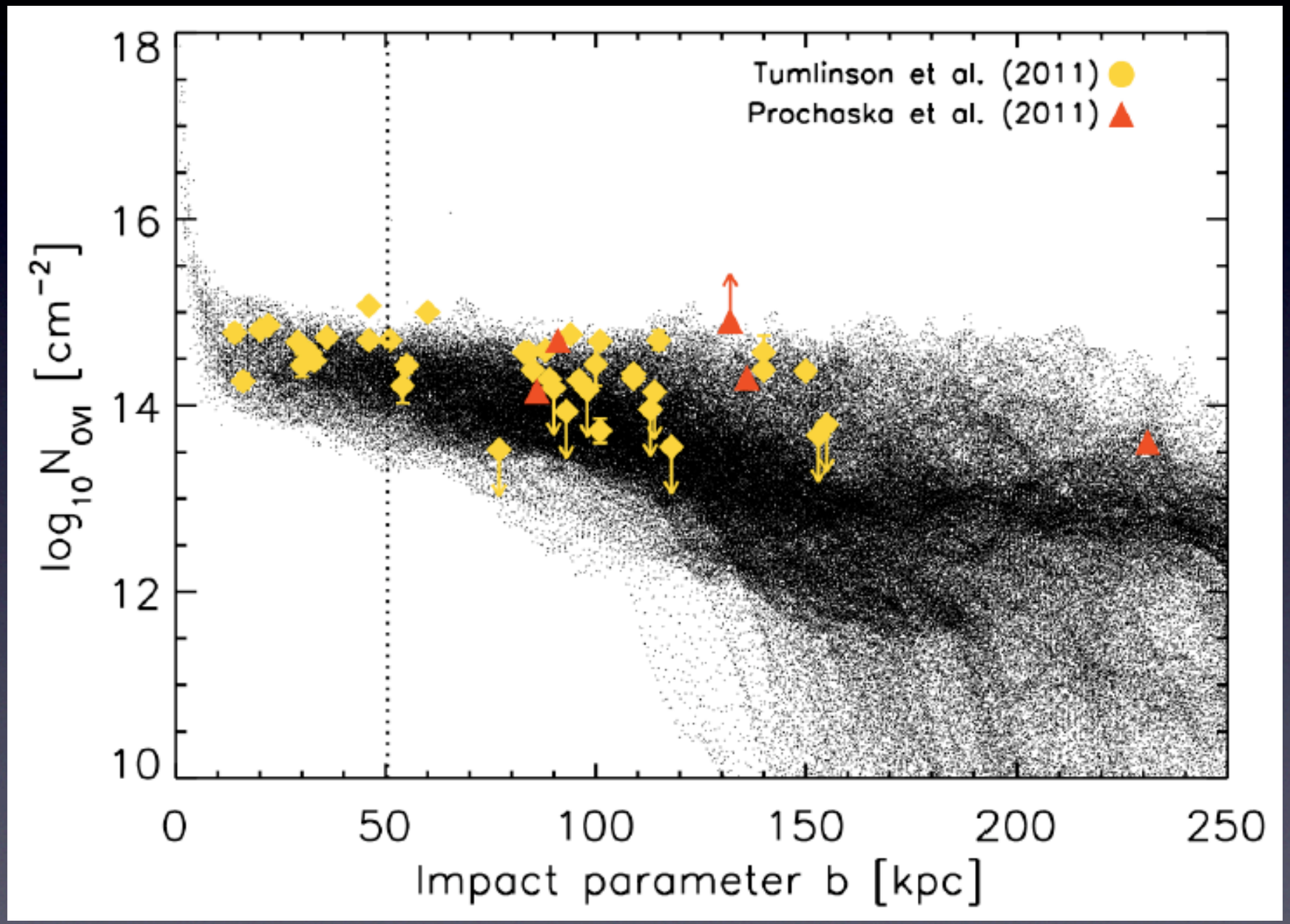

The Evolution of the CGM (Down to z=2.8)

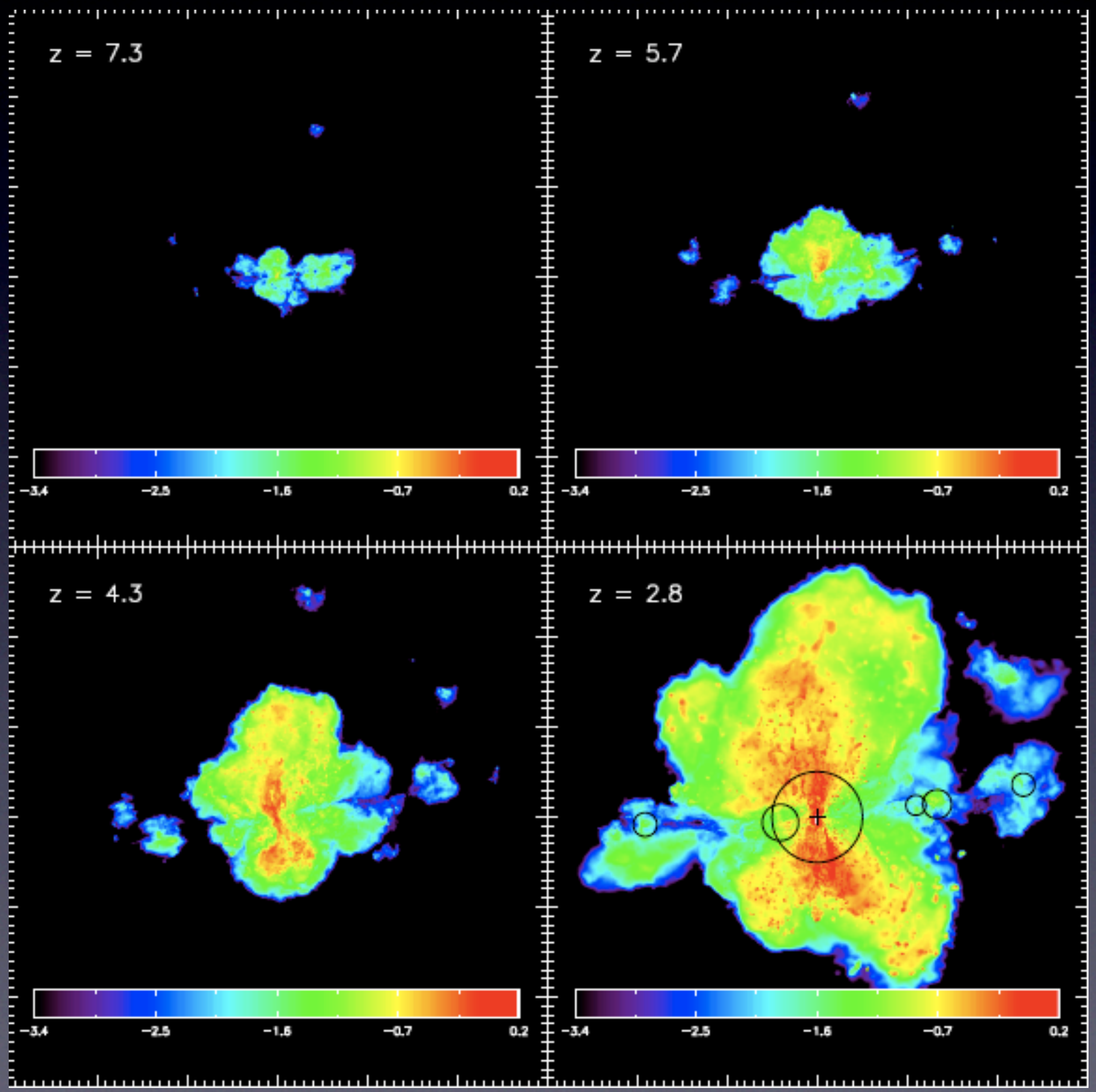

The Evolution of the CGM (Down to z=2.8)

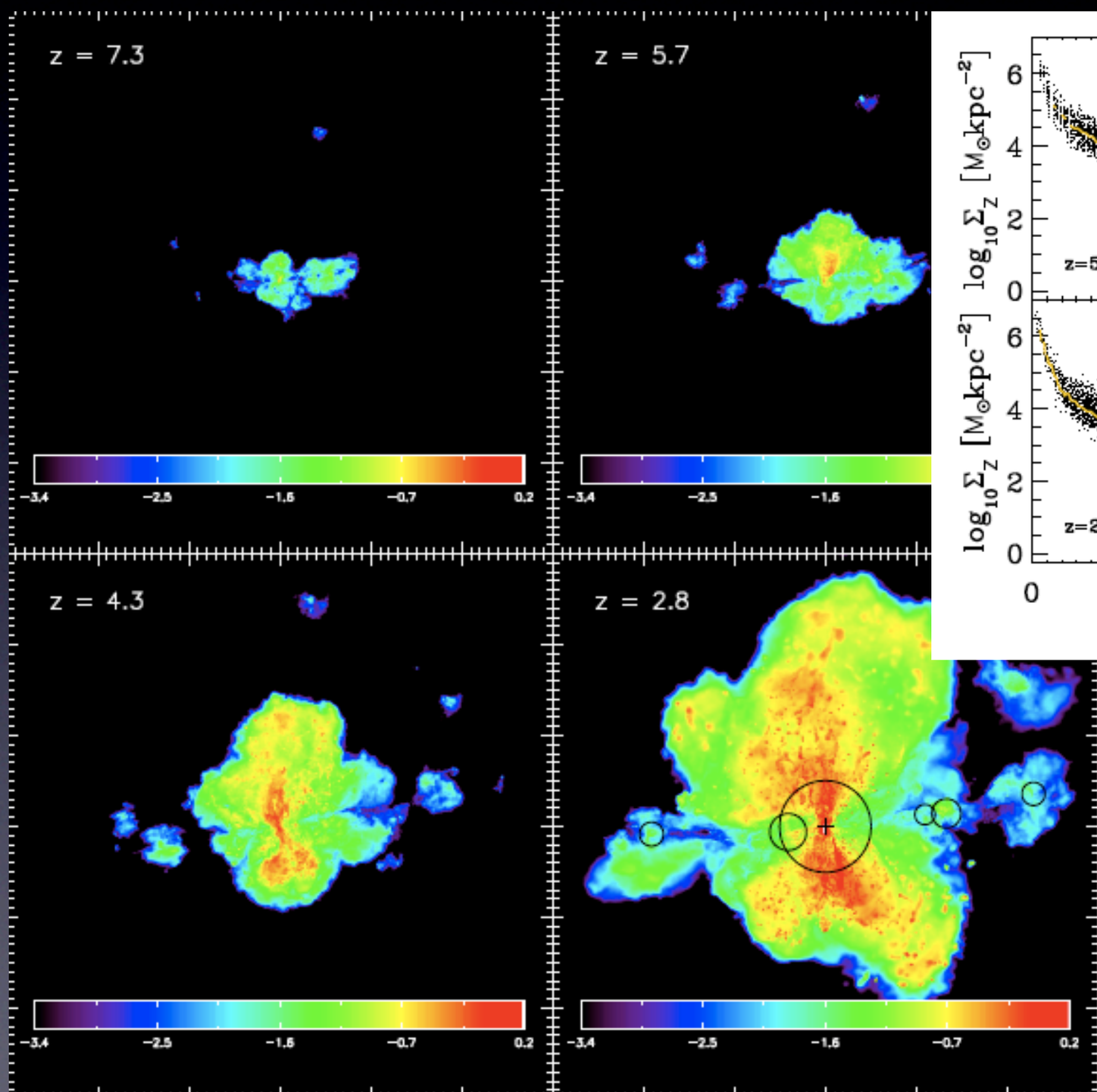

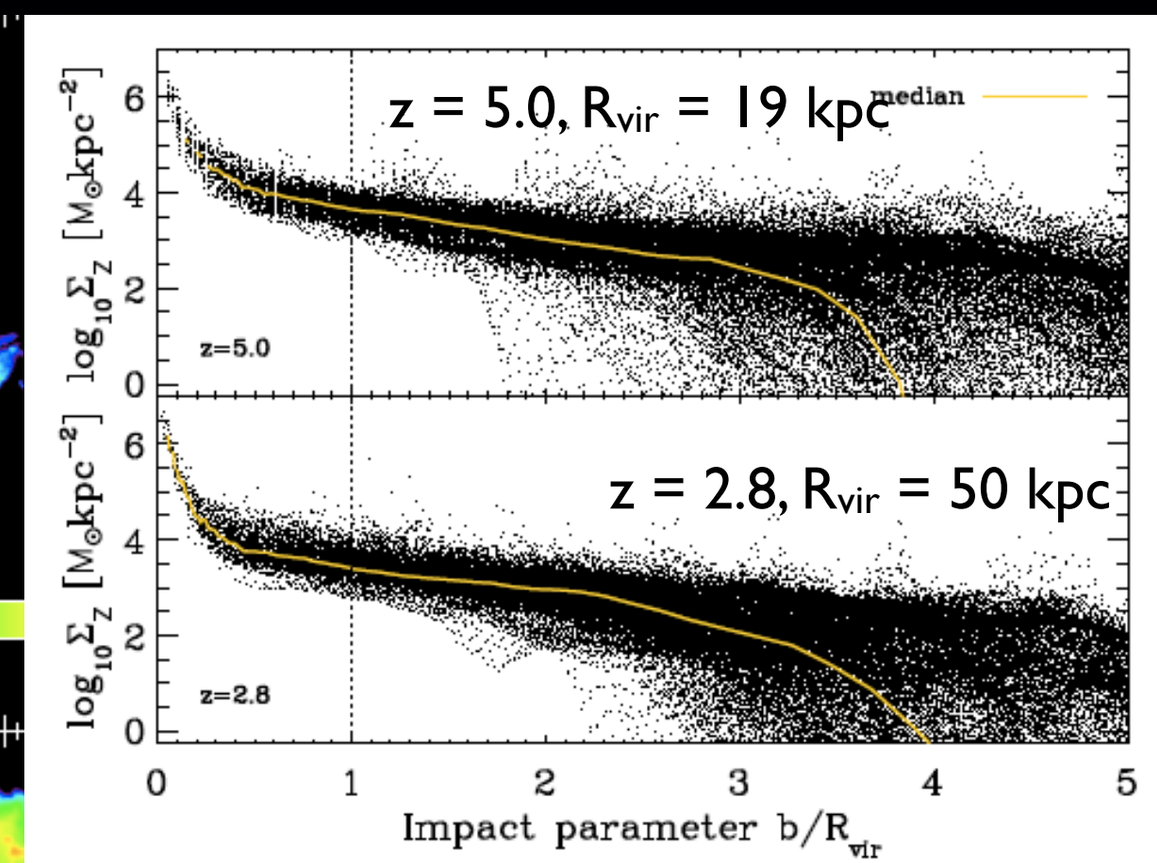

- From z = 7-8 to z ~ 3, the metal "bubble" grows with increasing R_{vir}
- z ~ 3 to z = 0?

Summary

- A comparison of the CGM properties between Eris2, a high resolution zoom-in simulation, and observations;
- Inflows and outflows coexist, about 1/3 of gas (by mass) within R_{vir} is outflowing, consistent with findings from cosmological simulations (van de Voort +2012);
- Low ions (Si II & C II): photoionized, $\delta > 100$, extends to 2 R_{vir}, but covering factor drops fast at $b > R_{vir}$
- High ions, in particular O VI, has *both* collisional ionized and photoionized components, depending on distance. *Large covering* factor with typical $N_{OVI} > 10^{14}$ cm^{-2}, consistent with the data from local starbursts (Tumlinson+2011, Prochaska+2012) .
- Synthetic spectra shows inflows and outflows are multi-phase, although not all the O_{VI} systems has corresponding low ion counterpart.
- W_0-b relation from Eris2 appears to be in good agreement of observations of Steidel +(2010). Feedback & outflows are important, however inflowing material contributes significantly to the absorption line strength.
- The covering factor of LLS system is about 27% within Rvir, in good agreement with Rudie+ (2012), it is slightly higher than, but consistent with simulations with no strong outflows (Fumagalli+ 2011; Faucher-Giguère & Kereš 2011); 90% of LLS within $2R_{vir}$ are inflowing cold streams.
- The cold streams (within 2 R_{vir}) are enriched to $Z > 0.01$ Z_{sun}, with typical value around 0.03 Z_{sun}, making the presence of cold stream detectable with metal absorption lines.

Backup Slides

Contribution of Host, Satellites Progenitors and Nearby Dwarf Galaxies

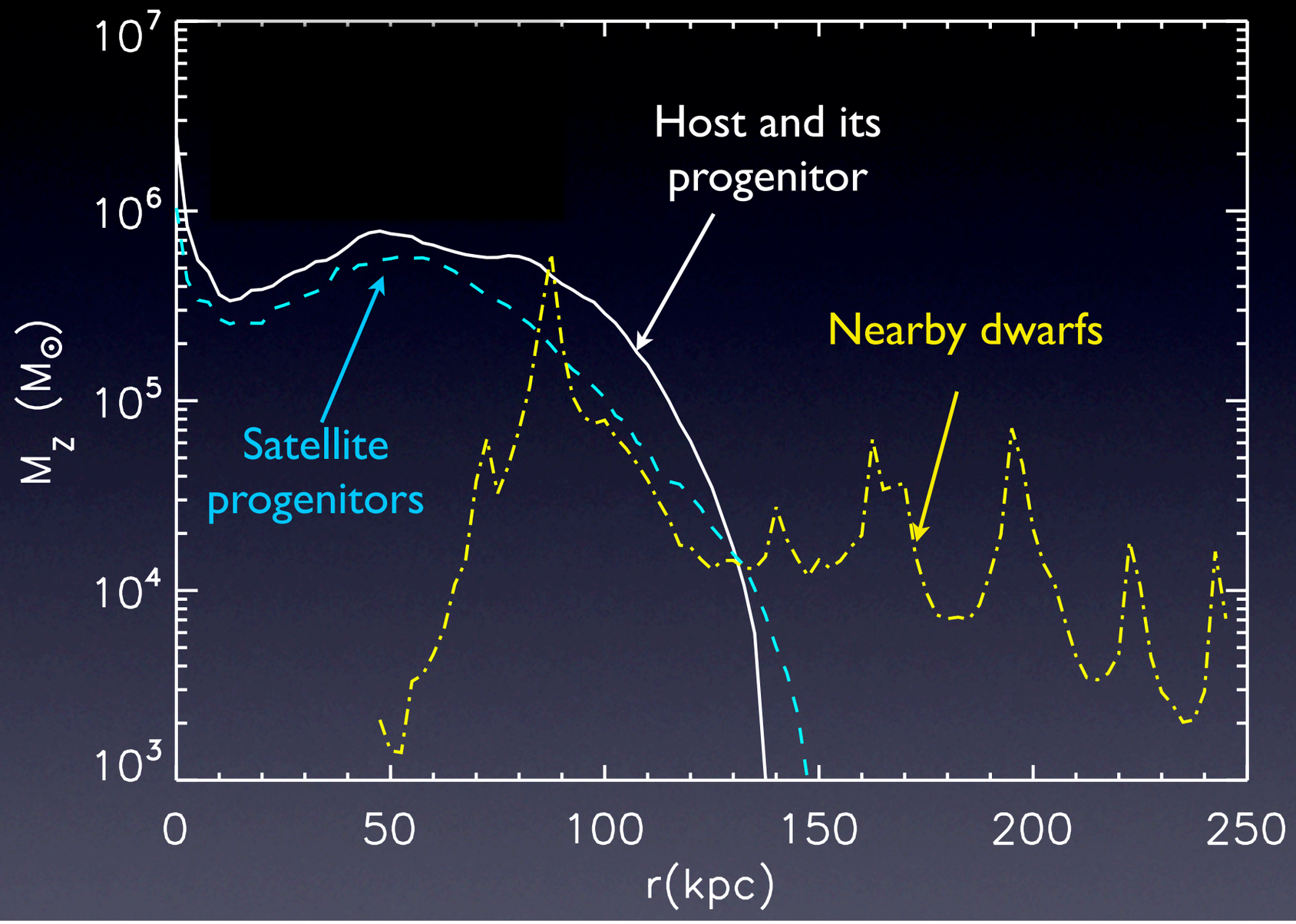

- Nearby dwarfs: satellite has not accreted yet at z = 3
- Progenitors: satellite has accreted by z = 3

	r ≤ Rvir	r ≤ 2 Rvir	r ≤ 3 Rvir	r > 3 Rvir
Host	61%	58%	58%	0
Sat. Progenitors	39%	38%	37%	3%
Nearby dwarfs	0	4%	5%	97%

Computing Fraction of Ions

- Post-processing using photo-ionization code Cloudy (Ferland+ 1998)
- Incident radiation includes the extragalactic UV background (Haardt & Madau 2012) and stellar UV
- Stellar UV radiation: using Starburst99 (Leitherer+ 1999), assuming a constant SFR of 20 M_{sun}/yr.
- Escape fraction f_{esc} = 3%, $J_d = J_0/(4\pi d^2)$
- Assuming gas is *optically thin:* not valid for column N_{HI} above LLS.

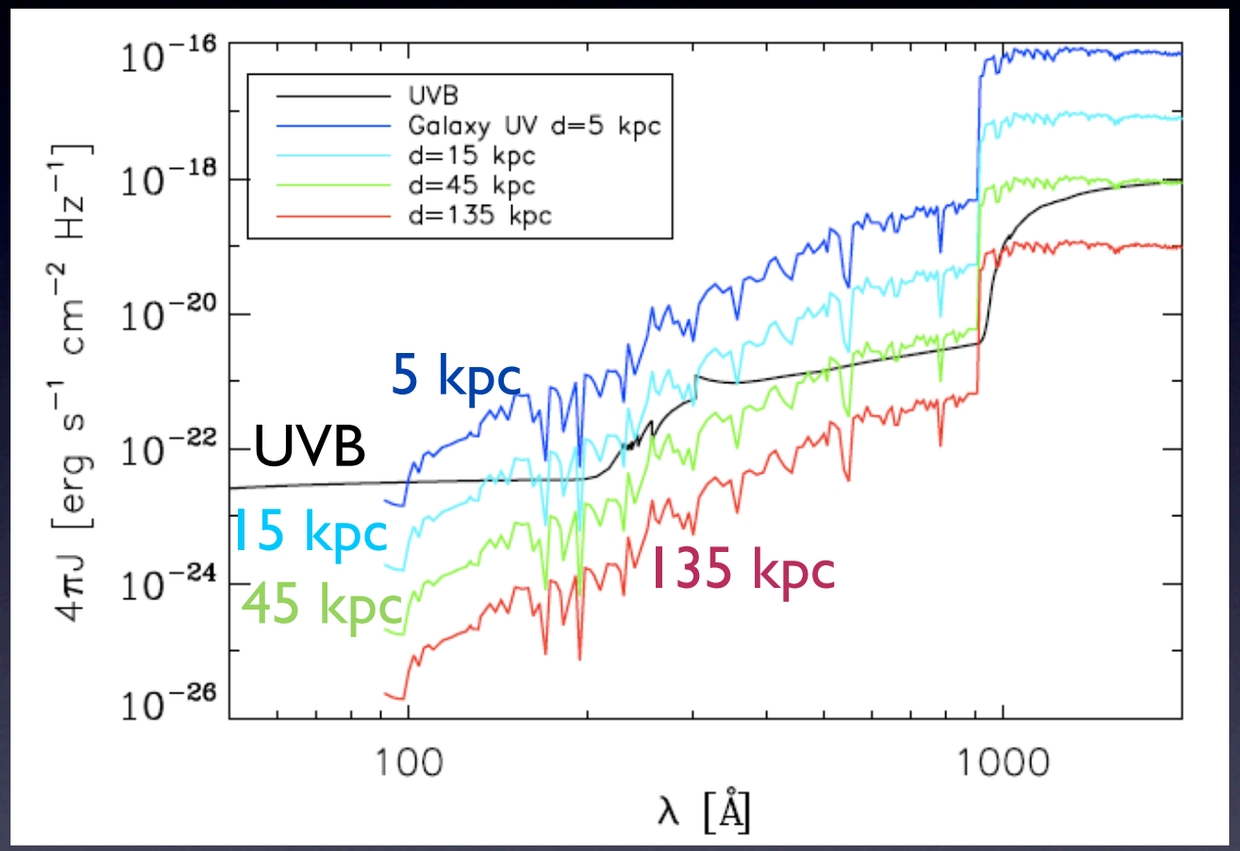

Photo-ionization heating due to local UV radiation is *not* taken into account.

The Effect of Gas Self-Shielding: Column density

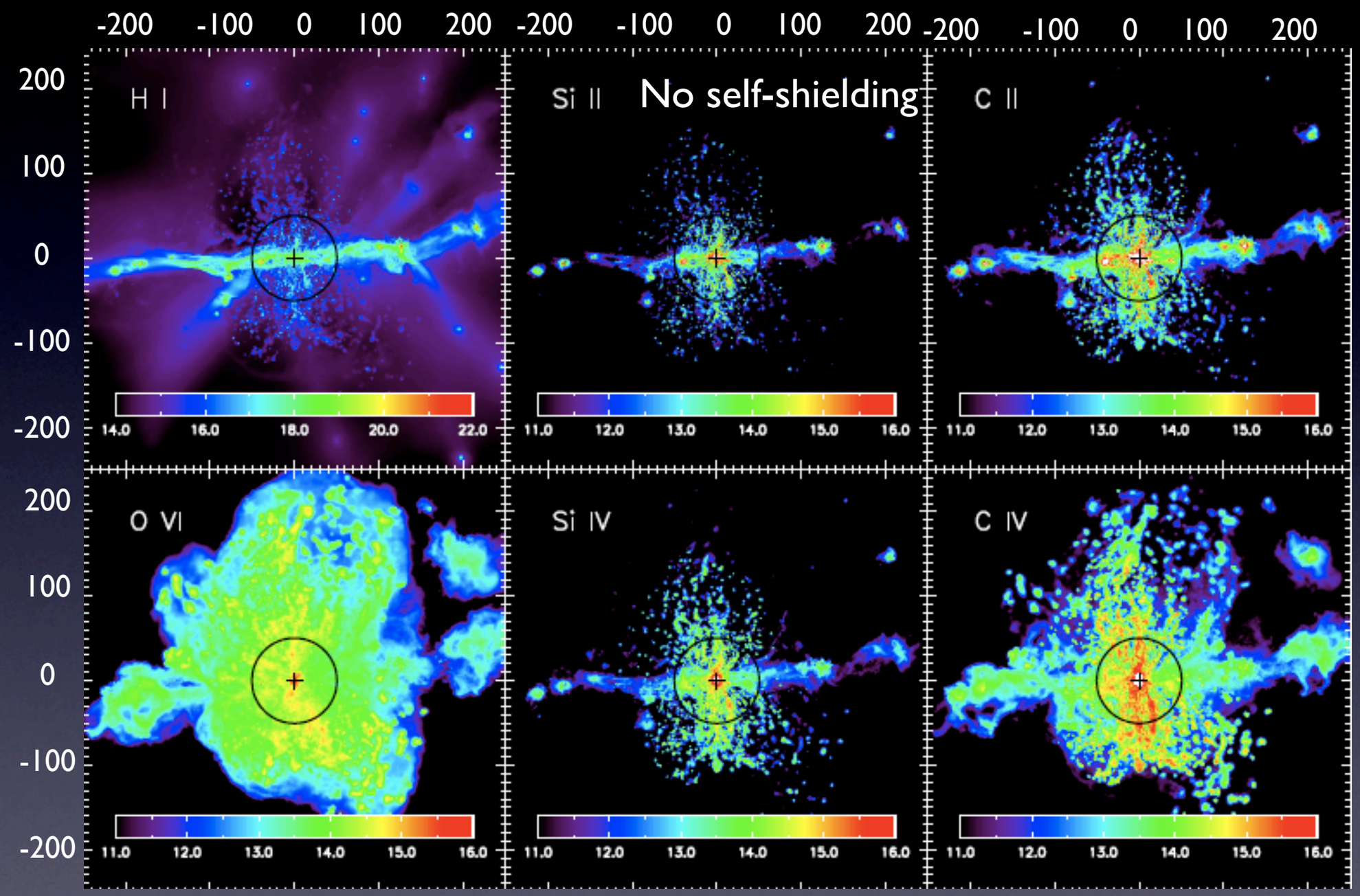

- Self-shielding approximation: for $n_H > 0.01$ cm^{-3}, the UV radiation rapidly decrease to zero, and ionization fraction recalculated in Cloudy. Except for the center region (< 10 kpc), the columns of metals are *not* significantly affected

The Effect of Gas Self-Shielding: Column density

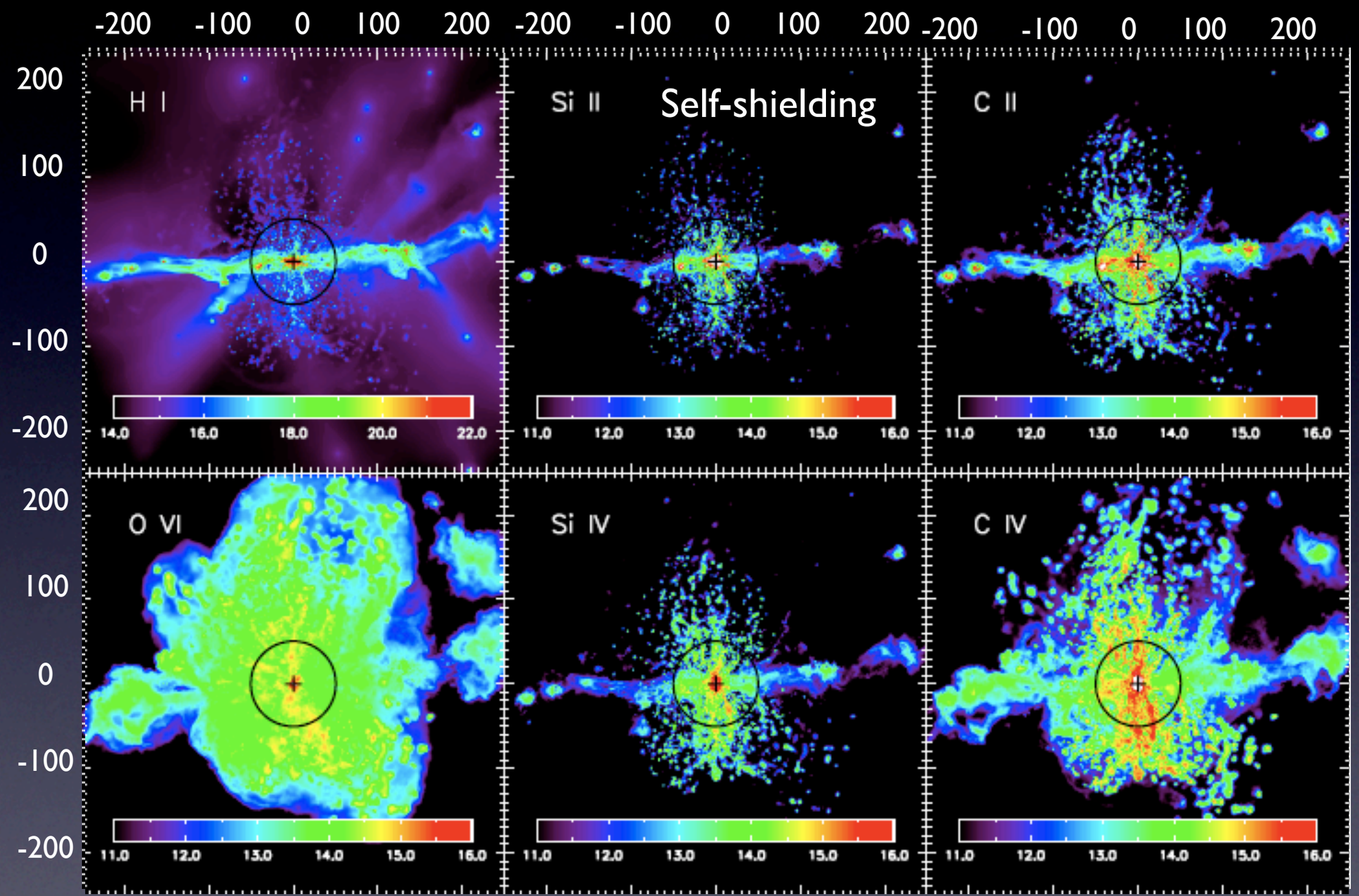

- Self-shielding approximation: for $n_H > 0.01$ cm^{-3}, the UV radiation rapidly decrease to zero, and ionization fraction recalculated in Cloudy. Except for the center region (< 10 kpc), the columns of metals are *not* significantly affected

The Effect of Gas Self-Shielding: W_0-b

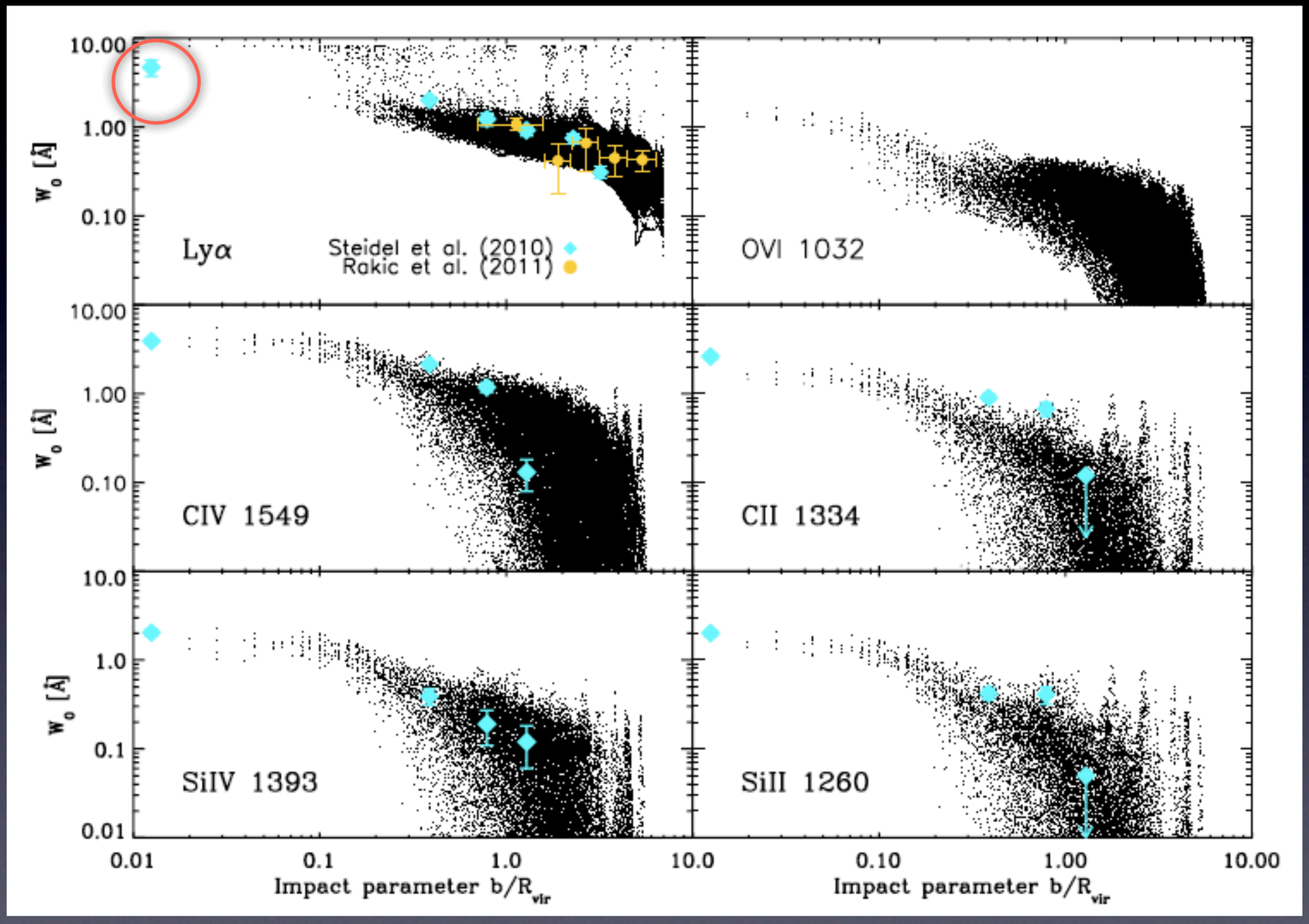

- Ly α: The data points within 5 kpc increases significant, W_0 become much higher than observations
- Metal lines: change is not significant since lines are saturated

Velocity Structure & Mass loading of Eris2

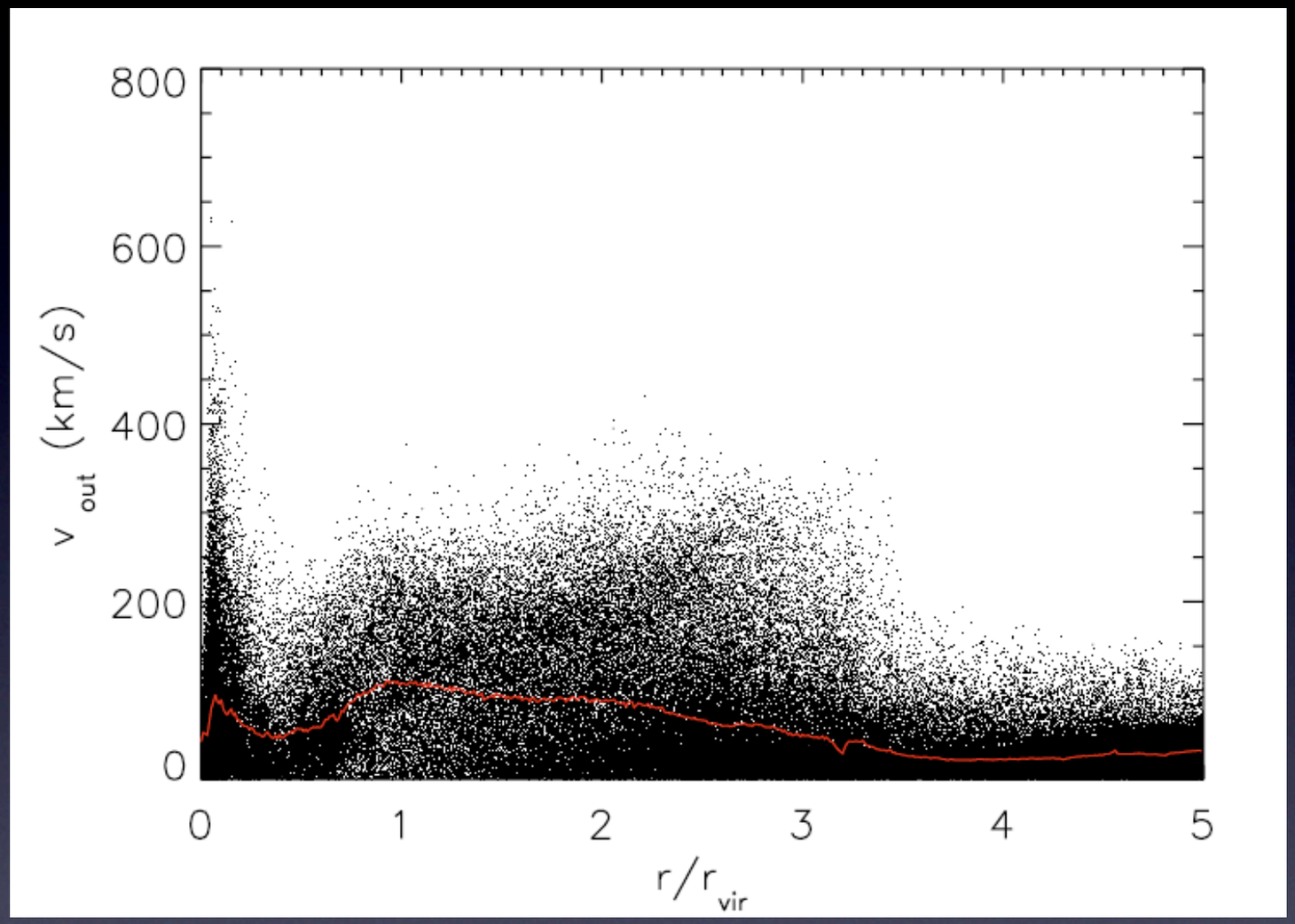

- Outflow gas mostly has v <~ 400 km/s, but can be up to ~ 700-800 km/s.
- Highest velocity gas is not reflected in the synthetic spectra because the column is very low

Eris vs. Eris2 at high Redshift: The Rotation Curve

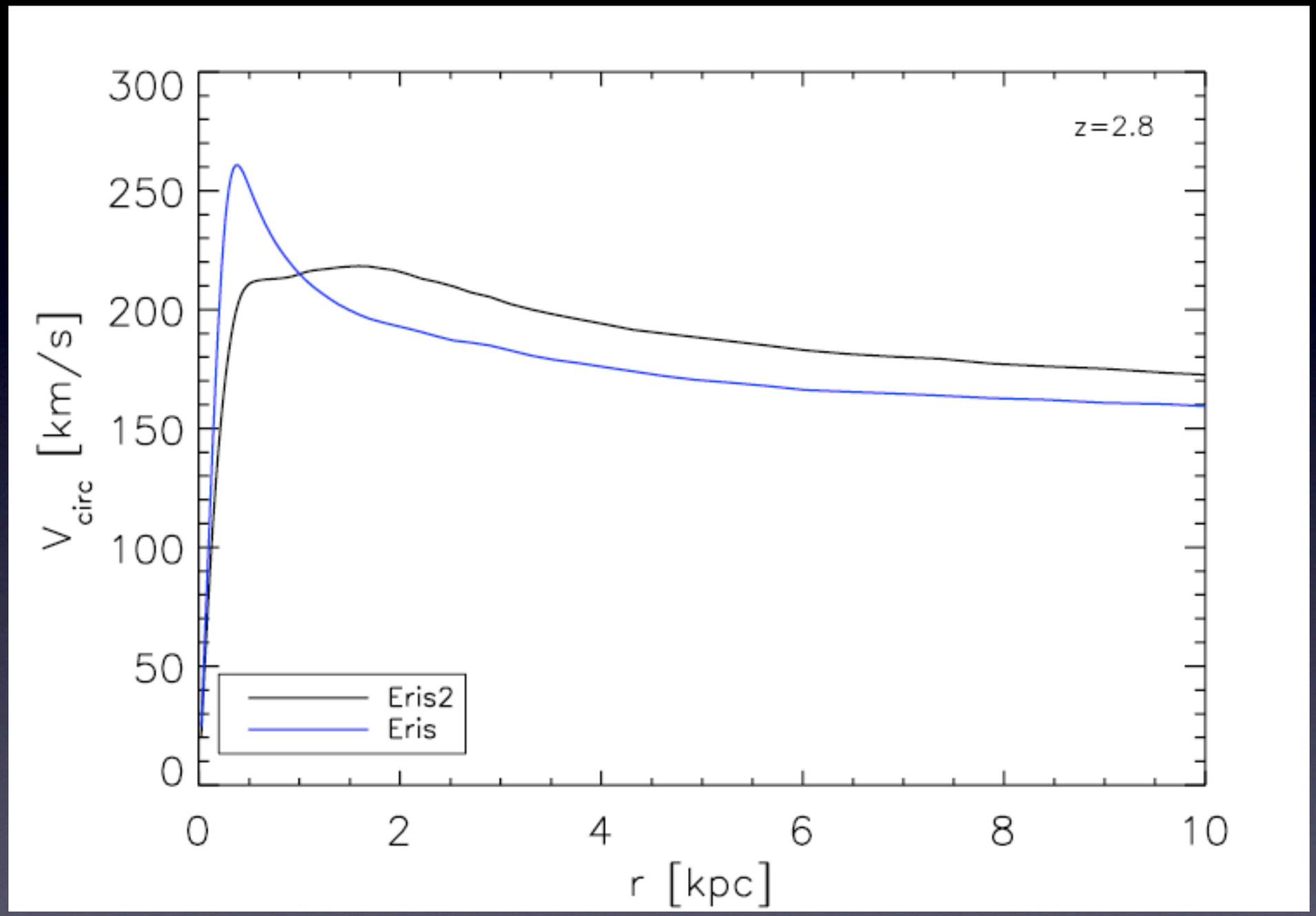

Nature of the Clumps & Possible Numerical Effects

Smagorinsky Model of Turbulent Diffusion

- Most basic turbulent model: (κ_{Turb} has units of velocity × length)

$$\frac{\partial \bar{u}}{\partial t} + \bar{v}.\nabla \bar{u} = -(\gamma - 1)\bar{u}(\nabla.\bar{v}) + \nabla \kappa_{Turb} \nabla \bar{u}$$

- Smagorinsky model (Mon. Weather Review 1963) -- Diffusion Coefficient determined by velocity Shear

$$\kappa_{Turb} = l_S^{\,2} S, \;\; S = \sqrt{S_{ij} S_{ij}}$$

- S_{ij} = trace-free strain rate of resolved flow; l_s = Smagorinsky length. For incompressible grid models $l_s^2 \sim 0.02\ \Delta x^2$

- For SPH we use $\kappa_{Turb} = C\ |S_{ij}| h^2$ with $C \sim 0.05$ (Wadsley, Veeravalli & Couchman 2008; See also Scannapieco & Brüggen 2008, Grief et al 2009)

- After implementation of turbulent diffusion, SPH is able to produce the entropy profile similar to grid codes

Effect of Turbulent Metal Mixing

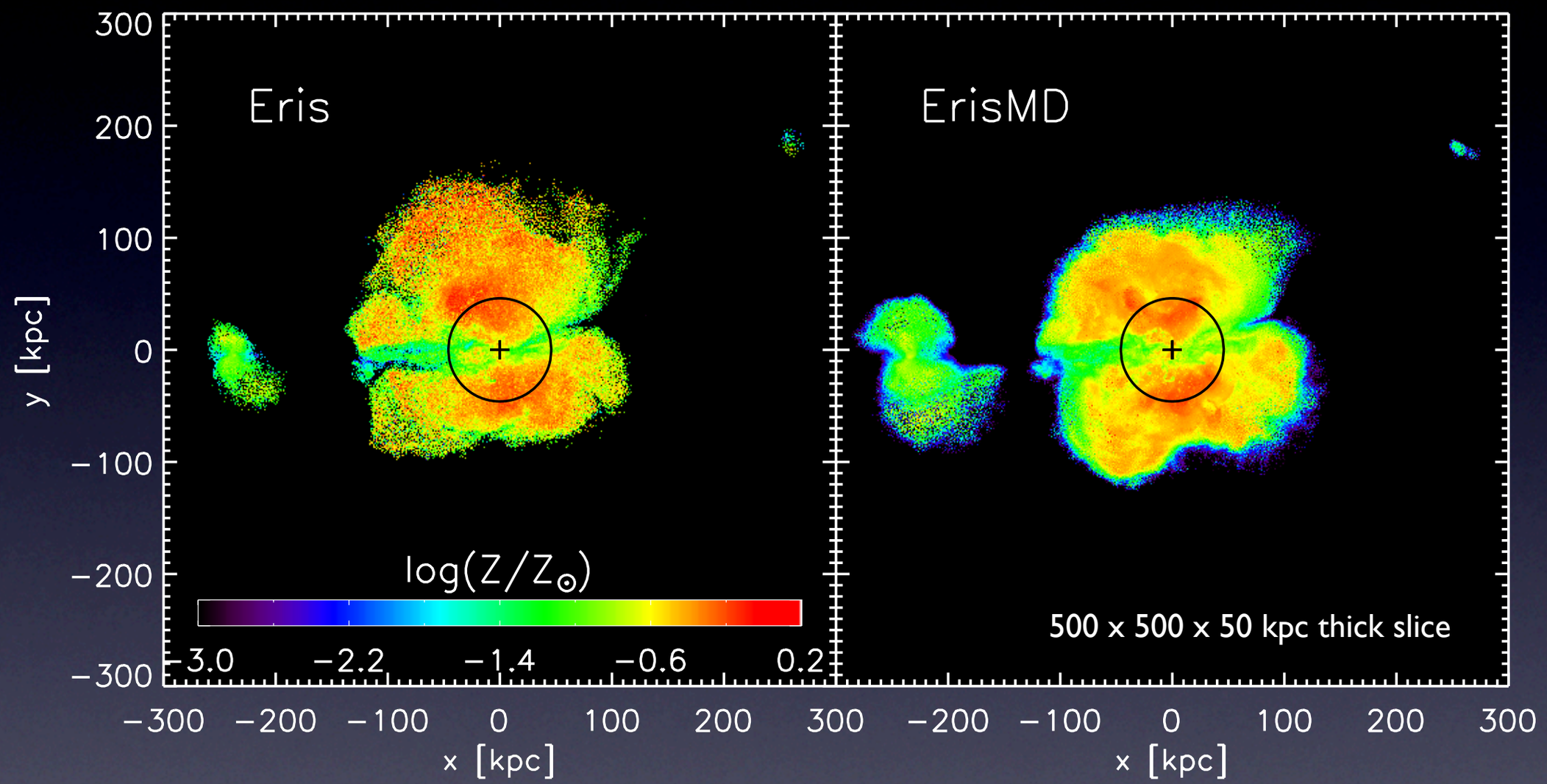

- SPH does not mix scalar quantities, metallicity 'locked' in gas particles
- ErisMD: same parameters as Eris but with a turbulent diffusion model (Shen et al. 2010). Simulation finish at z ~ 2.5.
- Smagorinsky model (Smagorinsky 1963): mixing proportional to velocity shear

Outflow Properties: Wind Speed

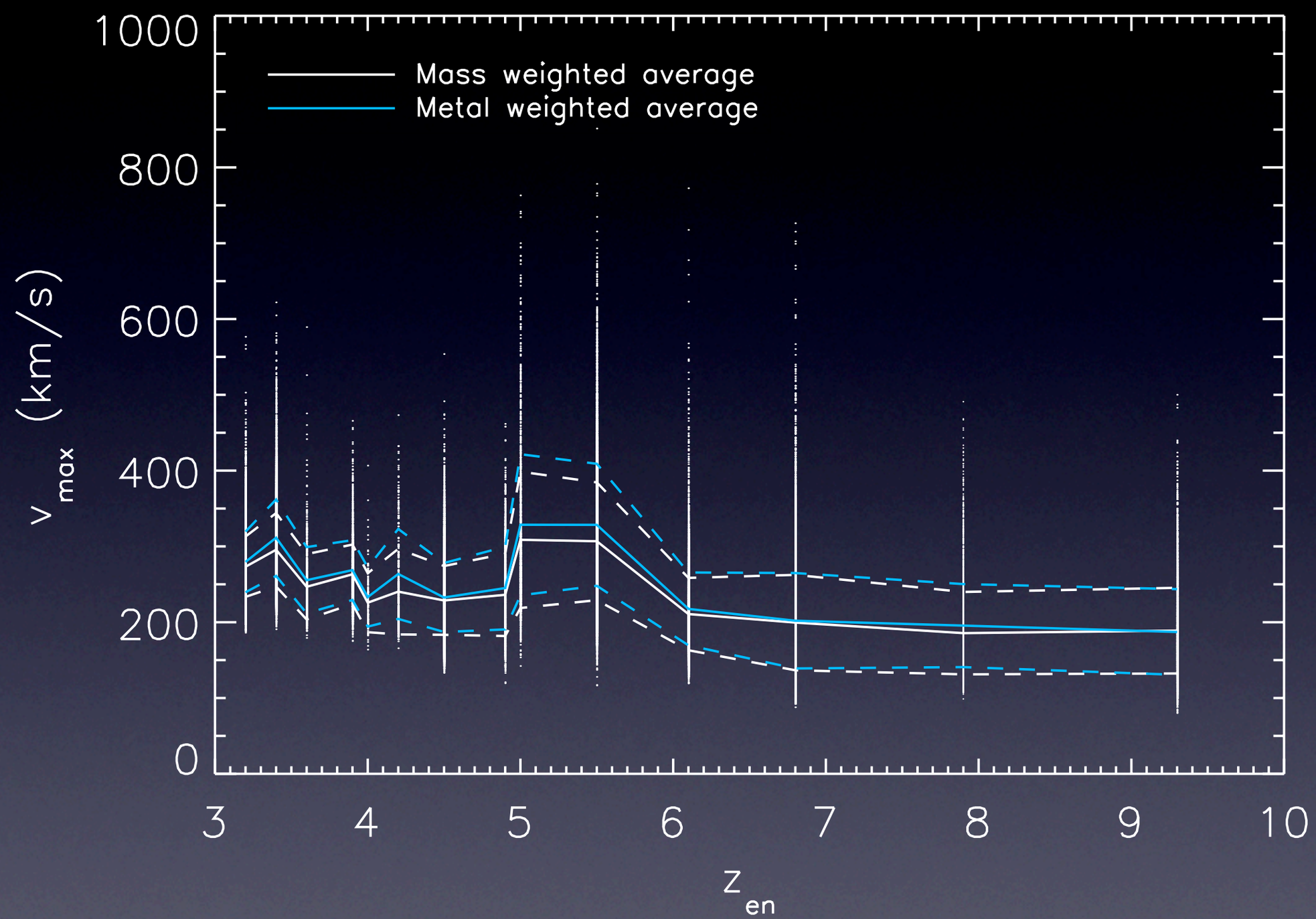

- Outflow radial velocity ~ 100-400 km/s, with maximum up to > 800 km/s;
- v_{eject} has no obvious relation with z (or M_{halo})